

# Compositional Trends for Total Vanadium Content and Vanadyl Porphyrins in Gel Permeation Chromatography Fractions Reveal Correlations between Asphaltene Aggregation and Ion Production Efficiency in Atmospheric Pressure Photoionization

Martha L. Chacón-Patiño, Rémi Moulian, Caroline Barrère-Mangote, Jonathan C. Putman, Chad R. Weisbrod, Greg T. Blakney, Brice Bouyssiere,\* Ryan P. Rodgers,\* and Pierre Giusti

Cite This: *Energy Fuels* 2020, 34, 16158–16172

Read Online

ACCESS |

Metrics & More

Article Recommendations

Supporting Information

**ABSTRACT:** Fourier transform ion cyclotron resonance mass spectrometry (FT-ICR MS) has exposed the ultracomplexity of fossil fuels, thereby validating the compositional trends that rule petroleum distillation, known as the *Boduszynski Continuum*. Routine FT-ICR MS analysis of a single crude oil sample can reveal tens-of-thousands of unique molecular formulas; however, currently available ionization methods suffer from limitations for such complex mixtures that are not yet completely understood. Simply put, MS detects ions, and thus, it depends heavily on the ability of ion sources to indiscriminately volatilize and subsequently ionize samples of interest. Despite advances in soft ionization methods, the characterization of complex matrices remains a challenge due to the lack of an ion source, commercial or custom-built, that can vaporize and ionize all compounds without bias, save analyte concentration. However, atmospheric pressure photoionization (APPI) has been shown to provide the most uniform ion production for mixtures of petroleum model compounds and real samples, with little to no fragmentation. In this work, we investigated the molecular composition of PetroPhase 2017 asphaltenes and its extrography fractions, with a focus on the total vanadium content and molecular composition of vanadyl porphyrins as a function of aggregate size distribution, accessed through separate experiments: online gel permeation chromatography (GPC) inductively coupled plasma–MS (ICP–MS) and online GPC APPI FT-ICR MS (at 21 T). The results reveal that the extrography separation provides asphaltene fractions (*i.e.*, acetone, Hep/Tol, and Tol/THF/MeOH) enriched in  $^{51}\text{V}$ -containing compounds with distinctive aggregate size distributions. The acetone fraction features smaller aggregate sizes, as it elutes later in the GPC chromatogram than Hep/Tol and Tol/THF/MeOH fractions, and overall, presents up to  $\sim 14$ -fold higher ionization efficiency in APPI. Such behavior suggests a correlation between aggregate size and production efficiency of monomeric ions in APPI. Bulk compositional trends accessed by GPC separation and highlighted by ICP–MS detection indicate that despite multiple separation steps (*i.e.*, extrography followed by GPC), APPI FT-ICR MS can only access  $\sim 37\%$  of the total V-containing compounds. Although the more stable/larger aggregates dominate the size distributions of all asphaltene samples studied, it is the weakly aggregated/monomeric species that are preferentially observed by APPI-MS. Tendencies in the molecular composition of vanadyl porphyrins and S/O-containing compounds strongly suggest that London forces might be central in the self-assembly process of asphaltene nanoaggregates to produce more massive clusters. The results demonstrate that the observed compositional trends (albeit limited) can be accessed when coupling advanced chromatographic separations with online high-field FT-ICR MS detection.

## INTRODUCTION

**“Classic” Asphaltene Chemistry.** Asphaltenes comprise arguably the most challenging and complex, naturally occurring mixture, and their importance to upstream production and downstream oil processing have triggered scientific interest for over 50 years.<sup>1–4</sup> Their definition as a solubility class, that is, *n*-heptane-insoluble/toluene-soluble, instead of a specific chemical/structural family, such as saturates, mono-aromatics, or vanadyl porphyrins, and associated complexity have motivated instrumentation advances in analytical chemistry, in particular, atomic force microscopy (AFM),<sup>5,6</sup> and high-magnetic field Fourier transform ion cyclotron resonance mass spectrometry (FT-ICR MS).<sup>7–9</sup>

The “modified Yen model” provides the most popular description of petroleum asphaltenes at the molecular level.

Mullins *et al.*<sup>3,10</sup> promoted the notion that asphaltenes are highly-aromatic/single-core molecules (known as “island”) that consist of  $\sim 7$  fused-aromatic rings and low number/length of alkyl-side chains. Based on bulk properties and low-resolution MS, the authors have suggested that the predominant intermolecular force in asphaltene self-assembly is  $\pi$ -stacking. They also concluded that heteroatom-based interactions, such as hydrogen bonding, have no overall effect in aggregation.<sup>11</sup>

Received: October 6, 2020

Revised: November 17, 2020

Published: December 7, 2020



The central concept of the modified Yen model is the stepwise association of monomeric species to form aggregates and then larger clusters, which is essentially a colloidal view.<sup>12</sup> These ideas have been recently supported by single-molecule AFM,<sup>5,6</sup> which revealed dominant island structures for various asphaltene samples. However, it is well known that AFM favors the detection of planar/near planar molecules.<sup>13</sup> Regardless of the limitations, some authors suggest that the island model is consistent with reservoir geodynamics,<sup>14,15</sup> but it is critical to point out that it fails to explain several asphaltene properties such as gas-phase fragmentation patterns in MS (tandem-MS),<sup>16,17</sup> the chemistry of thermal cracking products,<sup>18–20</sup> heterogeneous aggregation/solubility,<sup>21,22</sup> and interfacial behavior.<sup>23–25</sup>

**Role of FT-ICR MS in Modern Petroleomics.** High-field FT-ICR MS is widely viewed as the most advanced analytical tool for comprehensive molecular characterization of ultra-complex mixtures (e.g., crude oil, petroleum distillates, and dissolved organic matter) because of its inherent high resolution and accurate mass measurement capabilities that facilitate the assignment of individual elemental compositions to tens-of-thousands of species in a single sample in a matter of minutes by mass measurement alone.<sup>26,27</sup> For instance, McKenna *et al.*<sup>28</sup> reported the detection of ~85,000 species in a natural petroleum seep sample in which the authors identified nickel and vanadyl porphyrins with unprecedented mass accuracy. Recent works from the National High Magnetic Field Laboratory have highlighted the utility of the technique to investigate potential asphaltene structural motifs by tandem-MS, which demonstrated that single-core, “island” motifs coexist with those composed of multiple aromatic cores linked by covalent bonds (multicore or “archipelago”).<sup>29,30</sup> These findings were also supported by Wittrig,<sup>31</sup> Rüger,<sup>32–34</sup> Nyadong,<sup>35</sup> and Kenttämä *et al.*<sup>36</sup> Moreover, gas-phase fragmentation studies of geologically diverse asphaltene samples have revealed that the dominance of a particular structural motif (island or archipelago) is sample-dependent and correlates with the chemistry/structure of products from thermal cracking processes. These reports, along with recent findings by Xu,<sup>23,24,37</sup> Harbottle,<sup>38</sup> Clingenpeel,<sup>39</sup> and Jarvis *et al.*,<sup>40</sup> challenge the idea of the uniform dominance of highly aromatic/single-core structures in petroleum asphaltene samples and strongly suggest the existence of abundant multi-core “archipelago” species as well as heptane-insoluble/toluene-soluble compounds with “atypical” low aromaticity but high heteroatom content (*i.e.*, oxygen and sulfur).

**Limitations of MS.** Although MS has shed light on many of the compositional/structural trends that govern petroleum chemistry,<sup>41–44</sup> it suffers limitations (imposed by ionization methods) that are not entirely understood in complex matrices. Simply put, MS detects ions, and thus, it relies on the ability of ion sources to uniformly volatilize and ionize molecules within a complex sample. Development of “soft” ion sources, such as electrospray ionization (ESI), atmospheric pressure photoionization (APPI), and matrix-assisted laser desorption/ionization, has enabled the MS characterization of non-volatile/labile analytes from proteins to petroleum, creating the fields of proteomics and petroleomics.<sup>45–48</sup> However, the characterization of complex mixtures is still limited by selective ionization due to the absence of an ion source that can completely vaporize and ionize all compounds with no bias other than molar concentration. It is essential to point out that among all commercially available and custom-

built<sup>49–51</sup> ion sources capable of coupling to FT-ICR MS, APPI has been shown to provide the most uniform and complete ionization of mixtures of aromatic petroleum model compounds and real-world samples, with little or no fragmentation; it is hypothesized that some aliphatic species (e.g., cycloalkanes) exhibit lower ionization efficiency than aromatic compounds in APPI, but their response factor relative to aromatic species has not been determined.<sup>52,53</sup> For instance, Huba *et al.*<sup>54</sup> tested the ionization trends of a wide range of petroleum standards (e.g., naphthenic acids, 2–7 ring PAHs, nitrogen/sulfur-containing PAHs, furans, and phenols) in APPI, ESI, and atmospheric pressure chemical ionization (APCI). The authors concluded that APPI featured the lowest ion suppression effects, allowing the ionization of the broadest range of model compounds. In another work, Schrader *et al.*<sup>50</sup> used ESI, APPI, APCI, and custom-built atmospheric pressure laser ionization (APLI) to access the molecular composition of North American asphaltenes by FT-ICR MS. The authors concluded that APPI and APLI provided the broadest representation of asphaltenes, revealing the highest number of assigned molecular formulas and the closest H/C, O/C, and N/C ratios to bulk elemental analysis.

Early works by Cho *et al.*<sup>55</sup> demonstrated that petroleum MS characterization suffers considerable ion suppression effects. The authors fractionated an Arabian heavy oil into saturates, aromatics, resins, and asphaltenes and concluded that separate MS analyses enabled the identification of ~33,000 unique molecular formulas, compared with only ~18,000 species observed for the unfractionated/whole sample. Recently, Chacón-Patiño *et al.*<sup>30</sup> developed an extrography separation to improve the characterization of petroleum asphaltenes. The method involves asphaltene adsorption on silica gel and subsequent extraction with specific solvents. In the shortened version of the separation, the solid mixture of asphaltenes/SiO<sub>2</sub> is gradually extracted with acetone, Hep/Tol (1:1), and Tol/THF/MeOH (5:5:1). Although the solvent series seems unusual, it enables the initial isolation of highly aromatic/pericondensed structures, with high production efficiency of non-aggregated asphaltene ions in APPI, or high “monomer ion yield” (MIY), which leaves behind the asphaltene compounds that are more difficult to ionize as “monomeric” species. In brief, acetone is a polar solvent, but its predominant intermolecular interactions are dipole–dipole; thus, acetone selectively extracts alkyl-deficient polycyclic aromatic hydrocarbons (PAHs) and vanadyl porphyrins.<sup>56</sup> The second solvent mixture, Hep/Tol, assists the isolation of alkyl–aromatic compounds. Finally, Tol/THF/MeOH extracts the species that interact via hydrogen bonding with the SiO<sub>2</sub> silanol groups. MS and tandem-MS studies have demonstrated that asphaltene acetone fractions from diverse oils produce up to ~50-fold more monomeric ions and contain abundant single-core motifs. In contrast, Tol/THF/MeOH fractions are more difficult to ionize and comprise abundant multicore compounds. The authors performed heptane titrations of toluene solutions composed of the extrography fractions and observed increased precipitation (~2–10-fold) for the Tol/THF/MeOH fraction.<sup>29,30</sup> Thus, production efficiency of non-aggregated asphaltene ions in APPI, or MIY, was suggested to be affected by asphaltene aggregation. It is critical to point out that in those studies, naturally occurring vanadyl porphyrins (N<sub>4</sub>O<sub>1</sub><sup>51</sup>V<sub>1</sub> class) were utilized as naturally occurring internal standards; their gas-phase fragmentation was consistent with their known single-core structure.<sup>57</sup>

However, they were only detected in the acetone fractions from several different asphaltenes (e.g., Athabasca bitumen, South American heavy oils, Maya, and Arabian heavy), and it was not determined if difficult-to-ionize samples contain vanadium complexes locked into asphaltene aggregates.

**GPC to Correlate Petroleum Chemistry and Aggregation.** Online gel permeation chromatography (GPC) coupled to elemental analysis [inductively coupled plasma (ICP–MS)] has been useful to understand bulk compositional trends as a function of aggregate size distributions within petroleum samples.<sup>58–60</sup> Sulfur, vanadium, and nickel are usually monitored, and the resulting GPC ICP–MS chromatograms are commonly referred to as size profiles or size distributions.<sup>58,61</sup> Recent studies by GPC strongly suggest that London forces between aliphatic moieties have a central role in petroleum aggregation. For instance, Berruoco *et al.*<sup>62</sup> performed off-line characterization of GPC asphaltene fractions by synchronous UV–fluorescence spectroscopy and concluded that earlier-eluting fractions (most aggregated species) comprised compounds with high content of alkyl-side chains. Conversely, analysis of the later-eluting fractions (less aggregated asphaltenes/free molecules) revealed abundant alkyl-depleted/low-molecular-weight PAHs. In another work, Putman *et al.*<sup>63</sup> performed off-line FT-ICR MS characterization of GPC asphaltene fractions and observed that earlier-eluting compounds were more aliphatic, with MS-derived H/C ratios above 1.2. In contrast, later-eluting fractions revealed abundant highly-aromatic/alkyl-depleted species (H/C < 1.0). The authors observed similar trends for the parent whole crude oil, thereby suggesting that interactions between aliphatic moieties could be central in petroleum and asphaltene aggregation. These results are consistent with the idea that London forces between alkyl side chains drive the self-assembly of asphaltene nano-aggregates to produce more massive clusters, widely reported by Rogel,<sup>64</sup> Carbognani,<sup>65</sup> and Stachowiak *et al.*<sup>66</sup>

It is critical to point out that there is not a clear correlation between asphaltene aggregation in industrial applications (e.g., fouling in production facilities) and GPC elution trends. For example, Muller *et al.*<sup>67,68</sup> fractionated geologically diverse crude oils by GPC and used off-line FT-ICR MS for molecular characterization. The earlier-eluting fractions revealed abundant small aromatic cores (1–3 fused rings) with extensive alkyl substitution, whereas the later-eluting compounds were alkyl-depleted/sizable aromatic structures (5–9 fused rings). The authors suggested possible “non-size” effects for the later-eluting species, that is, the interaction of aromatic cores with the stationary phase. On the other hand, for the earlier-eluting fractions, the alkyl-side chains were suspected to prevent interactions between the aromatic cores and the column. Thus, alkyl-side chain content was suggested as the dominant molecular property that drives petroleum elution in GPC.

**Online GPC FT-ICR MS for Petroleum Analysis.** GPC fractionation with off-line FT-ICR MS detection is known to be limited by ion suppression effects and complicated by the potential presence of contaminants from repeated fraction collection/solvent evaporation.<sup>63,69</sup> Moreover, for vacuum residues and asphaltenes, it is increasingly difficult to determine if the observed ions reflect the real molecular composition of earlier-eluting/highly aggregated species.

Online molecular-level characterization has recently shown potential to mitigate the issues associated with fraction collection and off-line MS characterization.<sup>69</sup> There are few

reports about petroleum analysis by chromatographic methods with online FT-ICR MS detection.<sup>69,70</sup> The reason is simple: close mass splits such as 3.4 mDa (species differing in SH<sub>4</sub> vs C<sub>3</sub> content) and 1.1 mDa (<sup>13</sup>CH<sub>3</sub><sup>32</sup>S vs C<sub>4</sub>), abundant in heavy petroleum and asphaltenes, are a challenge to resolve on a chromatographic time scale. However, the custom-built 21 T FT-ICR mass spectrometer at the National High Magnetic Field Laboratory offers the most suitable option for online LC analysis because of its ultra-high resolving power,<sup>71</sup> mass accuracy, and sensitivity in a single scan, precluding the need for the coaddition of several scans required to yield sufficient resolving power and S/N.

In this work, the interlaboratory sample known as PetroPhase 2017 asphaltenes and its acetone, Hep/Tol, and Tol/THF/MeOH extrography fractions were fractionated by an improved GPC method that uses three columns in series to increase the resolution between earlier and later-eluting fractions. The GPC fractionation was hyphenated with positive-ion APPI 21 T FT-ICR MS characterization. Separate GPC <sup>51</sup>V ICP–MS studies were performed for quantification of total vanadium content as a function of aggregate size distribution. The results reveal that extrography yields asphaltene fractions that contain <sup>51</sup>V compounds with characteristic elution behavior in GPC. The acetone fraction elutes much later than Hep/Tol and Tol/THF/MeOH, and overall, features up to ~14-fold higher MIY (or ionization efficiency in APPI), which indicates that nanoaggregate size and production of monomeric ions are correlated. Bulk vanadium content, accessed by GPC ICP–MS, indicates that FT-ICR MS can only access up to ~37% of <sup>51</sup>V-containing compounds; the detected species are preferentially observed in the weakly aggregated GPC subfractions. The molecular composition of vanadyl porphyrins (N<sub>4</sub>O<sub>1</sub><sup>51</sup>V<sub>1</sub> class), along with S-containing compound classes, strongly suggest that London forces between aliphatic moieties might be central in asphaltene self-assembly.

## ■ EXPERIMENTAL METHODS

**Materials.** Asphaltenes were precipitated from an Arabian Heavy Petroleum sample (API = 29.2). High-performance liquid chromatographic (HPLC) grade *n*-heptane (Hep or C<sub>7</sub>), toluene (Tol), dichloromethane (DCM), acetone, and methanol (MeOH) were obtained from J.T. Baker and used as received. HPLC-grade tetrahydrofuran (THF) with no solvent stabilizer was purchased from Alfa Aesar. Filter paper Whatman 2, high purity microglass fiber thimbles, and chromatographic-grade silica gel (100–200 mesh, type 60 Å, Fisher Scientific) were used for asphaltene isolation from crude petroleum, asphaltene cleaning, and extrography fractionation.

**Asphaltene Precipitation and Extrography Fractionation.** Arabian heavy asphaltenes were prepared following a slightly modified version of the standard method D6560-12.<sup>72</sup> The prepared sample is known as “PetroPhase 2017 asphaltenes”.<sup>73</sup> In brief, petroleum was mixed with C<sub>7</sub> in a 1:40 ratio v/v. The dropwise addition of heptane was assisted by sonication (110 W, 40 kHz; Branson, Danbury, CT, USA) and refluxed heating at 90 °C for 2 h. The mixture was allowed to settle overnight; the precipitated solids were then collected by filtration (Whatman 2 filter paper). Asphaltenes were cleaned by extended Soxhlet extraction with C<sub>7</sub>, under N<sub>2</sub> atmosphere, until the solvent appeared colorless (~150 h). Asphaltenes were further washed by four cycles of crushing/Soxhlet extraction with heptane in order to decrease the concentration of occluded/coprecipitated maltenes. “Purified” asphaltenes were recovered by redissolution in hot toluene, dried under N<sub>2</sub>, and stored in the dark.

Asphaltenes were dissolved in DCM and mixed with silica gel (mass loading 1% = 10 mg of asphaltenes per gram of SiO<sub>2</sub>). The

mixture was dried entirely under  $N_2$  (24 h) and subsequently extracted in a Soxhlet apparatus with acetone, Hep/Tol (1:1, v/v), and Tol/THF/MeOH (5:5:1, v/v/v); each extraction lasts 24 h. The mixture asphaltenes/SiO<sub>2</sub> requires drying under  $N_2$  after each extraction step. The method is known as extrography and involves sample adsorption on a polar adsorbent (e.g., SiO<sub>2</sub>, alumina, and cellulose) and extraction with solvents of different polarity or varying intermolecular forces, such as acetone (dipole–dipole interactions) and THF/MeOH (hydrogen bonding).<sup>74</sup>

**GPC Coupled to ICP–Low-Resolution MS.** Mobile phase was delivered by a Dionex HPLC system equipped with an UltiMate 3000 microflow pump, an UltiMate 3000 autosampler, and a low port-to-port dead-volume microinjection valve. THF was used for sample preparation and mobile phase as it enables the highest sample recovery from the GPC columns (>99 wt %). A Styragel guard column (4.6 mm inner diameter, 30 mm length, 10,000 Da exclusion limit) was used before the GPC columns, and the chromatographic separation was performed by three GPC columns (from 1000 to 2,000,000 Da) connected in series. 100  $\mu$ L of asphaltene samples (5 mg/mL) was injected and eluted isocratically at 1 mL/min for 90 min. A post-column splitter was used to assure the infusion of 40  $\mu$ L/min into the ICP–MS. Samples were chromatographically separated and characterized as fresh solutions and prepared 1 h before analysis.

The ICP–MS (Thermo Scientific Element XR) was fitted with a modified DS-5 microflow total consumption nebulizer (CETAC, Omaha, NE), equipped with a custom jacketed glass spray chamber, as reported elsewhere. The spray chamber was thermostatted at 60 °C by a water bath circulator (Neslab RTE-111, Thermo Fisher Scientific, Waltham, MA). The ICP plasma conditions were Ar gas flow at 16 L/min, Ar auxiliary gas flow at 0.9 L/min, and Ar nebulizer gas flow at 0.6 L/min. O<sub>2</sub> (0.08 L/min) was used to avoid carbon deposition. The instrument was equipped with a quartz injector (inner diameter 1.0 mm), Pt sampler (orifice diameter 1.1 mm), and a skimmer with an aperture diameter of 0.8 mm. The ICP–MS was used to access the spectrally interfered isotopes of <sup>32</sup>S, <sup>51</sup>V, and <sup>58</sup>Ni. This work mainly focuses on <sup>51</sup>V content. Instrument conditions were optimized weekly by the use of a multielement tuning solution of Ag, Al, B, Ba, Ca, Cd, Co, Cr, Cu, Fe, In, K, Li, Mg, Mn, Mo, Na, Ni, P, Pb, Sc, Si, Sn, Ti, V, Zn, and Y in THF (1.0 ng/g). Mass offset was optimized daily and was applied to the data acquisition method to compensate the mass drift from the magnetic sector. Excel was used for the integration of the obtained chromatograms.

#### GPC Coupled to (+) APPI 21 T FT-ICR MS. GPC-FT-ICR-MS.

For ultra-high-resolution MS studies, the GPC separation was performed with an Alliance e2695 Separation Module (Waters Corporation, Milford, MA) equipped with the same set of three columns used for GPC ICP–MS. The HPLC system was operated with Empower 3 Chromatography Data Software. 100  $\mu$ L of asphaltene samples (5 mg/mL) was injected and eluted isocratically at 0.5 mL/min. All samples were separated/analyzed at 5 mg/mL. The effect of asphaltene concentration has been reported elsewhere.<sup>75</sup> The GPC effluent was split in 5, and 100  $\mu$ L/min was directly infused into the ion source. The APPI source (Ion Max, Thermo Fisher Scientific, San Jose, CA) was operated with a vaporizer temperature of 350 °C.  $N_2$  was used as sheath gas (50 psi) and auxiliary gas (32 mL/min) to prevent sample oxidation. Mass spectral analysis was performed with a custom-built 21 T FT-ICR mass spectrometer. Ion populations of  $1.5 \times 10^6$  charges were externally accumulated in a Velon Pro linear ion trap (Thermo Scientific, San Jose, CA) and ultimately transferred to a dynamically harmonized ICR cell operated with a trapping potential of 6 V.<sup>8,76</sup> Predator data station assisted MS data collection, with 3.1 or 6.2 s transient duration during the chromatographic time frame. These conditions provide a mass resolving power of  $\sim 3,400,000$  at  $m/z$  400 for a single phased (absorption mode) mass spectrum, facilitating the resolution of the 1.1 mDa mass split ( $SH_3^{15}C$  vs  $^{12}C_4$ ) at  $m/z > 800$ . The large ion population used here is possible only due to the high magnetic field and yields high dynamic range per single scan without compromising the spectral acquisition rate. This promotes the highest chromatographic resolution since spectral averaging is not required. Ion

injection times (ITs) were metered by automated gain control (AGC). AGC is a well-described process in which the linear radio frequency ion trap performs a very brief pre-scan to determine the instantaneous flux of ions. This measurement is extrapolated to determine the ion IT required to meet the user defined AGC target (specified in number of fundamental charges). In this study, the AGC target was  $1.5 \times 10^6$  charges. Predator Software assisted data collection, phase-correction, and internal calibration with abundant hydrocarbon homologous series.<sup>77</sup> PetroOrg Software assisted molecular formula assignment and data visualization by plots of double bond equivalents (DBE = number of rings plus double bonds to carbon) versus carbon number.<sup>78</sup>

## RESULTS AND DISCUSSION

### GPC ICP–MS Chromatograms for Asphaltene Extrography Fractions.

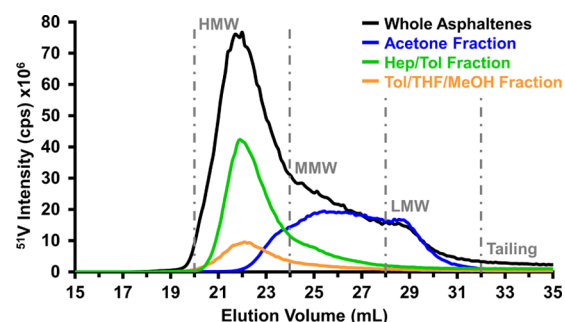


**Figure 1.** <sup>51</sup>V GPC ICP–MS chromatograms for whole PetroPhase 2017 asphaltenes (black) and its extrography fractions: acetone (blue), Hep/Tol (green), and Tol/THF/MeOH (orange). High, medium, and LMW, and tailing elution ranges are highlighted by gray dashed lines.

chromatograms for whole PetroPhase 2017 asphaltenes and its acetone, Hep/Tol, and Tol/THF/MeOH extrography fractions. This analytical approach allows for the quantitative determination of <sup>51</sup>V-containing nanoaggregate size distributions, along with other metals or heteroatoms such as <sup>58</sup>Ni and <sup>32</sup>S. The highlighted elution ranges (gray dashed lines) have been previously defined based on the molecular weight distribution of polystyrene standards (e.g., high molecular weight > 10,000 Da, medium molecular weight  $\sim 1000$ –10,000 Da, low molecular weight < 1000 Da) and comprise<sup>61,75</sup> high molecular weight (HMW, 20–24 mL elution volume), medium molecular weight (MMW, 24–28 mL), and low molecular weight (LMW, 28–32 mL) species, plus a “tailing” fraction (>32 mL). It is essential to point out that in this study, adsorption effects or strong interaction between asphaltenes and the GPC column have not been considered; therefore, HMW species are assumed to be sizable/stable aggregates, whereas LMW and tailing compounds are ascribed to weakly aggregated or asphaltene “monomers” (free molecules). The tailing fraction, more abundant for the whole sample, comprises non-aggregated vanadium compounds that elute after the full permeation volume and might experience strong adsorption on the stationary phase. It is important to highlight that the V-containing tailing fraction is less pronounced for the extrography fractions. We hypothesize that this behavior is likely due to (1) absence of those compounds due to their irreversible retention on the silica gel particles used for the extrography separation and (2) possible cooperative stabilization between asphaltene fractions when they are part of the

whole sample. Collection of the GPC fractions (e.g., HMW and tailing), followed by solvent evaporation, dilution, and reinjection into the GPC separation system, yielded a nanoaggregate distribution similar to that obtained when the whole sample was injected (i.e., HMW and tailing). Moreover, we have used three GPC columns in series, which enables higher chromatographic resolution and observation of multimodal size profiles, compared to the monomodal-like distributions previously reported by Putman *et al.*<sup>69,79</sup>

The size distribution of the whole PetroPhase 2017 asphaltenes (black) indicates a diverse population of <sup>51</sup>V-containing aggregates. The integrated areas of the GPC chromatograms are presented in Table 1 and facilitate sample

**Table 1. Integrated Areas (%) for the GPC <sup>51</sup>V ICP–MS Chromatograms for Whole PetroPhase 2017 Asphaltenes and Its Acetone, Hep/Tol, and Tol/THF/MeOH Extrography Fractions**

sample	prior to HMW <sup>a</sup> (%)	HMW (%)	MMW (%)	LMW (%)	tailing (%)
whole PetroPhase 2017 asphaltenes	0.90	59.00	27.06	9.94	3.09
acetone fraction	0.03	13.06	60.70	24.82	1.39
Hep/Tol fraction	0.20	72.91	19.02	4.39	3.48
Tol/THF/MeOH fraction	1.12	66.47	21.20	6.87	4.34

<sup>a</sup>Fraction eluted before the established molecular weight ranges. Material can elute before the defined MW ranges.

comparison. For whole asphaltenes, ~59, 27, and 10% of the total area correspond to HMW, MMW, and LMW species, plus a ~3% for the tailing region. Thus, the size GPC profiles for the extrography fractions indicate that the separation reported by Chacón-Patiño<sup>29</sup> yields asphaltene cuts with distinctive aggregation behavior.<sup>80</sup> The acetone fraction, previously shown to contain abundant single-core (island) motifs with a high production efficiency of non-aggregated ions in APPI, or high MIY, mostly reveals MMW (~61%) and LMW (~25%) vanadium-containing species, whereas Hep/Tol and Tol/THF/MeOH fractions, shown to be enriched in multicore (archipelago) structures with a much lower MIY,<sup>29</sup> mostly elute in the HMW region (73/66%).

In previous work, we accessed the precipitation behavior by titration and the molecular composition via direct-infusion (+) APPI FT-ICR MS, of whole PetroPhase 2017 asphaltenes and its extrography fractions. The results suggested a stronger precipitation tendency in heptane/toluene mixtures for Hep/Tol and Tol/THF/MeOH, whereas acetone featured up to ~20-fold higher stability.<sup>29,80</sup> Thus, ionization efficiency in APPI was linked to asphaltene precipitation, and strong aggregation (low concentration of monomeric species) was suggested as the reason for poor ionization efficiency. Furthermore, <sup>51</sup>V-containing compounds, or vanadyl porphyrins (N<sub>4</sub>O<sub>1</sub><sup>51</sup>V<sub>1</sub>) as revealed by (+) APPI FT-ICR MS, were only detected in the acetone fraction. Therefore, the aggregation trends presented in Figure 1 agree with the previously reported precipitation behavior in bulk liquid phase. However, the results here demonstrate that <sup>51</sup>V-containing compounds are present in all extrography fractions; GPC elution trends suggest that lack of observation in direct infusion MS experiments is likely due to a prominent aggregation tendency.

**GPC Hyphenated to Positive-Ion APPI 21 T FT-ICR MS.** The GPC separation system was coupled with an APPI ion source operated in positive mode attached to a custom-built 21 T FT-ICR mass spectrometer. The instrument is equipped with AGC,<sup>8</sup> which determines an appropriate *ion accumulation period* to hit a constant target ion population ( $1.5 \times 10^6$  charges),<sup>81</sup> required for optimal data collection, for each scan during the entire chromatographic run. Figure 2, upper

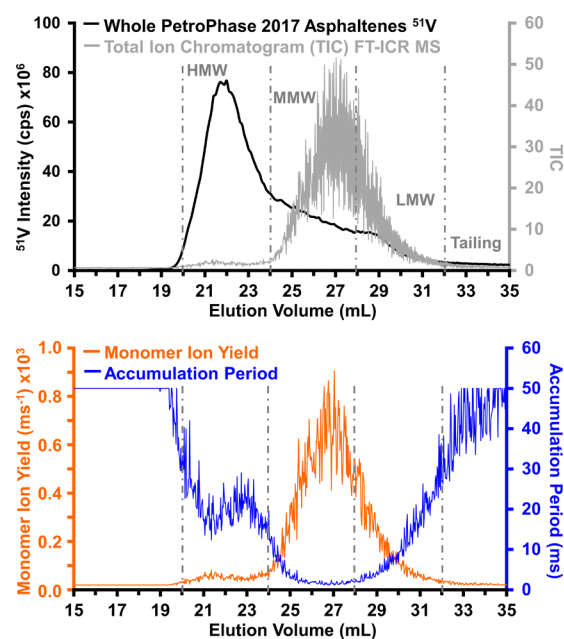


**Figure 2.** Upper panel: <sup>51</sup>V GPC ICP–MS chromatogram for whole PetroPhase 2017 asphaltenes (black) plotted along with the total IC (TIC) derived from (+) APPI 21 T FT-ICR MS (gray). Lower panel: accumulation period (ms) required to hit the target of  $1 \times 10^5$  charges (blue) and MIY, (orange) throughout the entire GPC separation.

panel, presents the total ion chromatogram (IC) for whole PetroPhase 2017 asphaltenes (gray) measured by (+) APPI FT-ICR MS and also shows the GPC <sup>51</sup>V ICP–MS chromatogram (black) for comparison. Although the sample comprises ~59% of <sup>51</sup>V-containing HMW compounds (ICP data, integrated areas, Table 1), the total ion current (TIC) is maximum for the MMW species, close to the LMW region limit. Figure 2, lower panel, features the accumulation period (blue) for the whole chromatographic separation, which maxed out for the HMW region, and the elution volumes for which the <sup>51</sup>V content, as determined by GPC ICP–MS, are low (<20 mL and tailing). Figure 2, lower panel, also presents the MIY (orange) as a function of elution volume. MIY is calculated by eq 1 and is consistent with the TIC. The results suggest an inverse correlation between the production efficiency of monomeric ions, MIY, and aggregate size.

$$\text{MIY} = \frac{1}{\text{accumulation period}} \times 1000 \text{ (ms}^{-1}\text{)} \quad (1)$$

**Correlation between Aggregation Trends and Production Efficiency of Monomeric Ions in APPI.** Figure 3, left panel, presents the MIY (orange) as a function of elution volume for the PetroPhase 2017 asphaltenes extrography fractions; the values are derived from (+) APPI FT-ICR MS (eq 1). Acetone features the most optimal ionization: the MMW species exhibit up to MIY ~2100. Conversely, Hep/Tol

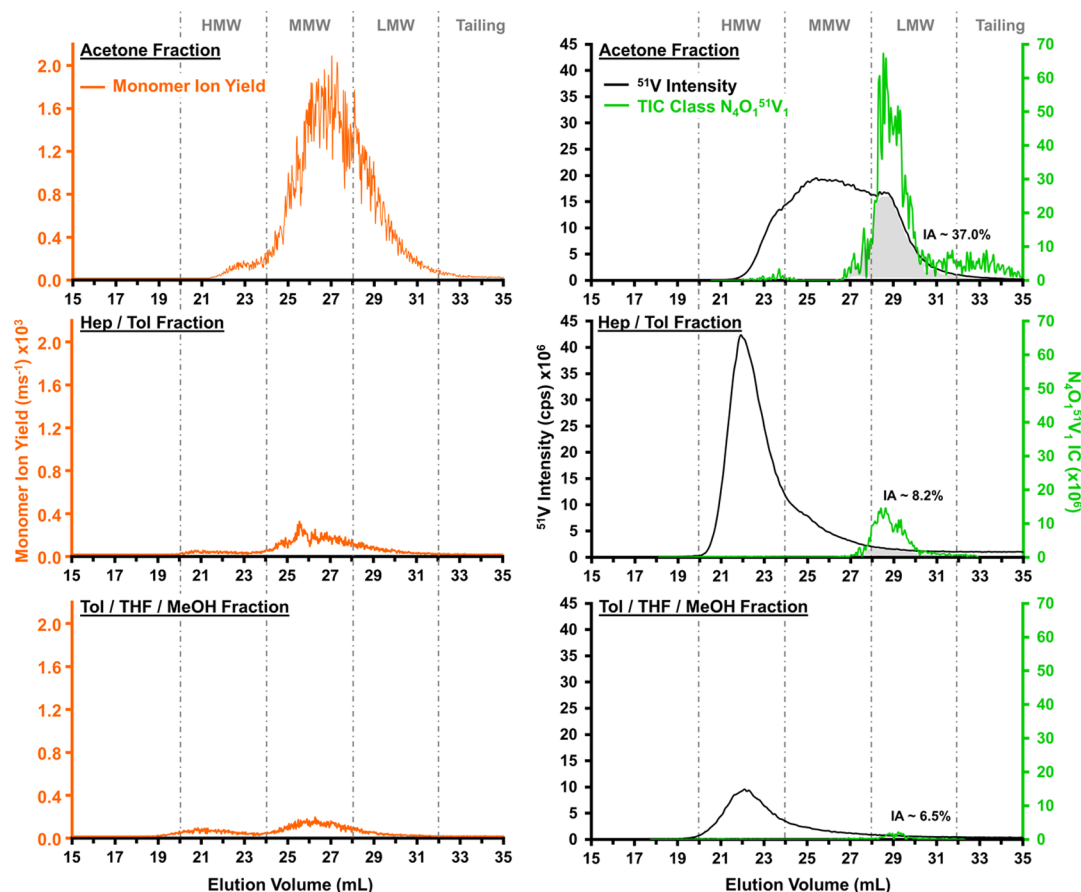


**Figure 3.** Left: MIY, as a function of elution volume, for the extrography fractions from PetroPhase 2017 asphaltenes. Right: GPC  $^{51}\text{V}$  ICP–MS chromatograms (black) plotted along with the ICs for vanadyl porphyrins ( $\text{N}_4\text{O}_1^{51}\text{V}_1$  class, green). IA are highlighted and suggest that detected  $\text{N}_4\text{O}_1^{51}\text{V}_1$  species by (+) APPI FT-ICR MS may correspond to  $\sim 37.0$ ,  $8.2$ , and  $6.5\%$  of the total vanadium content detected via ICP–MS. Abundant  $^{51}\text{V}$ , as measured by ICP, and its limited detection in (+) APPI FT-ICR MS, demonstrate an inverse correlation between aggregate size and MIY.

and Tol/THF/MeOH fractions present a poor production of monomeric ions, with a  $\sim 7$ – $14$ -fold lower MIY for the elution volumes in which ion accumulation time maxed out. Although most of Hep/Tol and Tol/THF/MeOH  $^{51}\text{V}$ -containing species elute in the HMW region ( $\sim 73/66\%$  integrated areas), the results suggest that most of the ions derive from MMW and LMW GPC subfractions.

Molecular formulas assigned to the mass spectral peaks based on accurate mass are sorted in compound classes. For instance, all the formulas with carbon, hydrogen, and one sulfur atom comprise the class  $\text{S}_1$ . Thus, vanadyl porphyrins, with one oxygen, one vanadium, and four nitrogen atoms, make up the class  $\text{N}_4\text{O}_1^{51}\text{V}_1$ . Porphyrins with additional heteroatoms, for example,  $\text{N}_1\text{O}_1\text{S}_1^{51}\text{V}_1$ , previously reported by Gray,<sup>82</sup> Qian,<sup>83</sup> and McKenna *et al.*,<sup>84</sup> are in much lower concentration and are the topic of future work. Figure 3, right panel, presents the IC for the  $\text{N}_4\text{O}_1^{51}\text{V}_1$  class (green) for all the extrography fractions and again, their GPC  $^{51}\text{V}$  ICP–MS chromatograms (black) for comparison. The whole sample is included in the Supporting Information Figure S1.  $\text{N}_4\text{O}_1^{51}\text{V}_1$  species were mostly detected in the LMW and tailing acetone subfractions, despite the majority of the  $^{51}\text{V}$ -containing compounds eluted in the MMW region ( $\sim 61\%$ , integrated area–ICP–MS), which indeed, presents the highest MIY values. The intersection area (IA) between  $^{51}\text{V}$  ICP–MS and  $\text{N}_4\text{O}_1^{51}\text{V}_1$  FT-ICR MS ICs is highlighted in Figure 3 (gray)

and can be used to qualitatively infer the observation window of (+) APPI FT-ICR MS. The results suggest access to only  $\sim 37.0\%$  of the total vanadium content of the acetone fraction. The later extrography fractions follow the same trend: although  $73/66\%$  of Hep/Tol and Tol/THF/MeOH species elute in the HMW region, most of the vanadyl porphyrins are detected in the LMW aggregates, and the IAs suggest minimal APPI-MS access to  $^{51}\text{V}$ -containing compounds ( $\sim 8.2$  and  $\sim 6.5\%$ ).

Collectively, the results support the notion that GPC can be used to access asphaltene aggregation trends, as the results are consistent with previously reported precipitation/deposition behaviors.<sup>29,85</sup> Lack of FT-ICR MS detection of abundant  $\text{N}_4\text{O}_1^{51}\text{V}_1$  compounds in the HMW region, despite the high  $^{51}\text{V}$  abundance revealed by ICP–MS, confirms that APPI FT-ICR MS analysis of asphaltenes is strongly hampered by aggregation.

**Molecular Composition as a Function of Aggregate Size Distribution.** Molecular formulas can be sorted by the number of rings and double bonds (DBE) respective to carbon atoms. Figure 4, upper panel, presents the DBE versus carbon number plots for the  $\text{N}_4\text{O}_1^{51}\text{V}_1$  class for the GPC subfractions from whole PetroPhase 2017 asphaltenes. In these graphs, the color scale represents the relative abundance, normalized within each class for each GPC subfraction. Thus, in Figure 4, the molecular formulas and contour plots result from coadding the scans collected for the corresponding HMW, MMW,

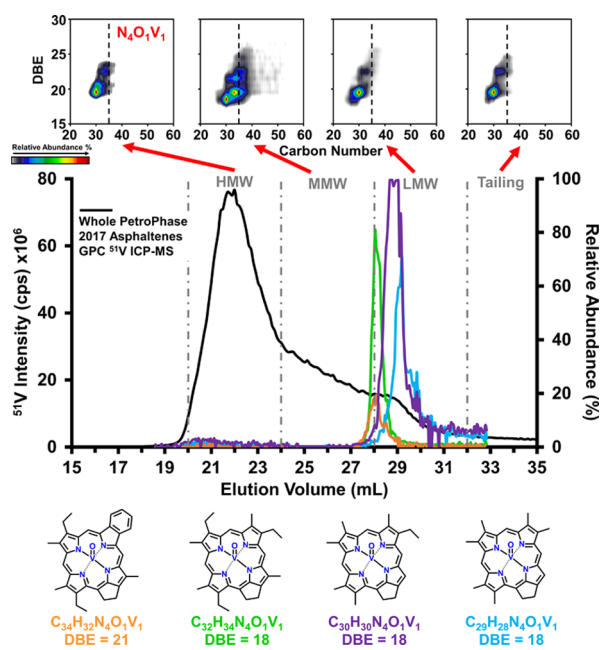


**Figure 4.** DBE vs carbon number plots for the  $N_4O_1V_1$  class for the various GPC regions from whole PetroPhase 2017 asphaltenes (upper panel) and relative abundance as a function of elution volume for the most abundant  $N_4O_1V_1$  formulas (middle panel). Data derived from (+) APPI FT-ICR MS characterization. The GPC  $^{51}V$  ICP-MS chromatogram (black) is included for reference, and the most likely molecular structures for the most abundant vanadyl porphyrins are presented in the lower panel.

LMW, and tailing GPC regions. Furthermore, compounds with the same DBE but varying content of carbon number belong to the same homologous series.

In Figure 4, it is important to keep in account that vanadyl porphyrins eluted as HMW aggregates exhibit a global relative abundance below 2%; these species reveal a narrow distribution of carbon number ( $\sim 28$ – $35$ ). We hypothesize that these compounds may exist as “free” porphyrins available on the surface of sizable aggregates and thus remain accessible

to APPI FT-ICR MS. Conversely, the abundant  $N_4O_1V_1$  species detected in the MMW GPC fraction (up to  $\sim 60\%$  of relative abundance, green line) reveal more extended homologous series (carbon number  $\sim 27$ – $50$ ), which translates into a higher content of carbon atoms in alkyl-side chains. Finally, the disaggregated/monomeric compounds, LMW/tailing subfractions, exhibit abundant  $N_4O_1V_1$  species with decreased alkylation (carbon number  $\sim 27$ – $35$ ). We hypothesize that these compounds are likely “free” porphyrins and thus their molecular composition could hint correlations between GPC elution trends and molecular structure. As discussed above, “tailing” species may also experience adsorption on the stationary phase and therefore elute after the full permeation volume. The global compositional trends are consistent with the results reported by Putman *et al.*,<sup>63,69</sup> who concluded that the most abundant species in larger aggregates (e.g., MMW) contain more carbon atoms in alkyl-side chains, suggesting that London forces may be fundamental in asphaltene self-association. Several reports<sup>22,86–89</sup> suggest extensive trapping/occlusion of porphyrins within asphaltene aggregates, which is consistent with the abundant detection of vanadium-containing compounds in large/sizable aggregates in this work.

Figure 4, middle panel, presents the relative abundance of the most abundant  $N_4O_1V_1$  molecular formulas as a function of elution volume, plotted along with the GPC  $^{51}V$  ICP-MS chromatogram for comparison. The lower panel features the most likely molecular structure for the most abundant species.<sup>90–92</sup> Although the differences in carbon number and DBE are minimal, the results suggest a good chromatographic resolution between the  $N_4O_1V_1$  species highlighted in orange/green and purple/blue. The results also indicate that the GPC elution of non-aggregated species is ruled by the presence of side groups (either alkylic or aromatic). More substituted compounds elute earlier, which suggests that steric hindrance around the porphyrin core might prevent a stronger interaction/longer residence period in the stationary phase. Previous studies indicate that the GPC elution order of metal porphyrins mostly depends on the molecular geometry and the presence of exocyclic rings.<sup>93,94</sup> For instance, the vanadyl group ( $V=O$ ) produces a pyramidal geometry with the porphyrin

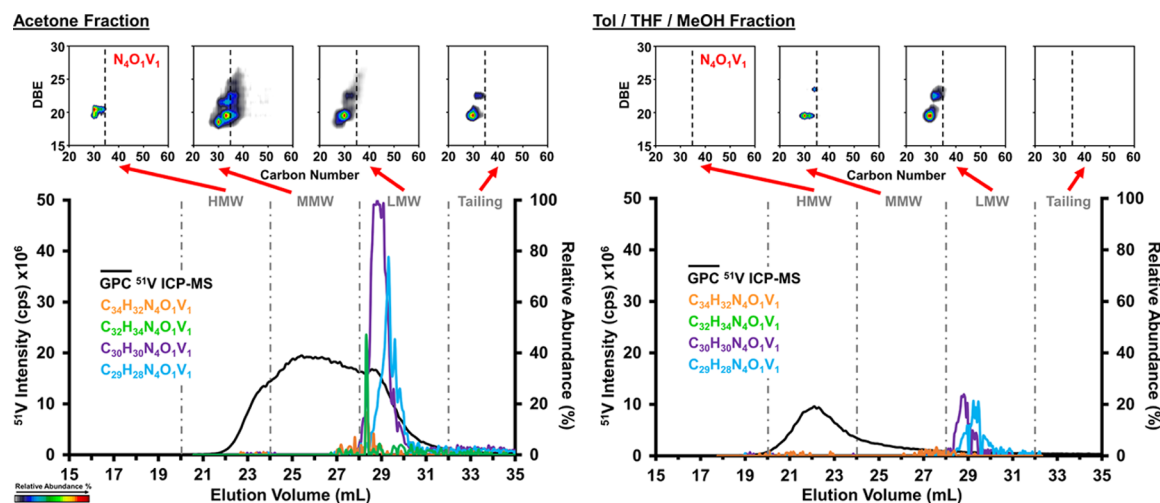


**Figure 5.** Upper row: DBE vs carbon number plots for the  $N_4O_1V_1$  class for all GPC subfractions from acetone (left) and Tol/THF/MeOH (right) extrography fractions from PetroPhase 2017 asphaltenes. Data derived from (+) APPI 21 T FT-ICR MS characterization. Lower row: relative abundance, as a function of elution volume, for the most abundant  $N_4O_1V_1$  molecular formulas. The GPC  $^{51}V$  ICP-MS chromatogram (black) is included for reference.

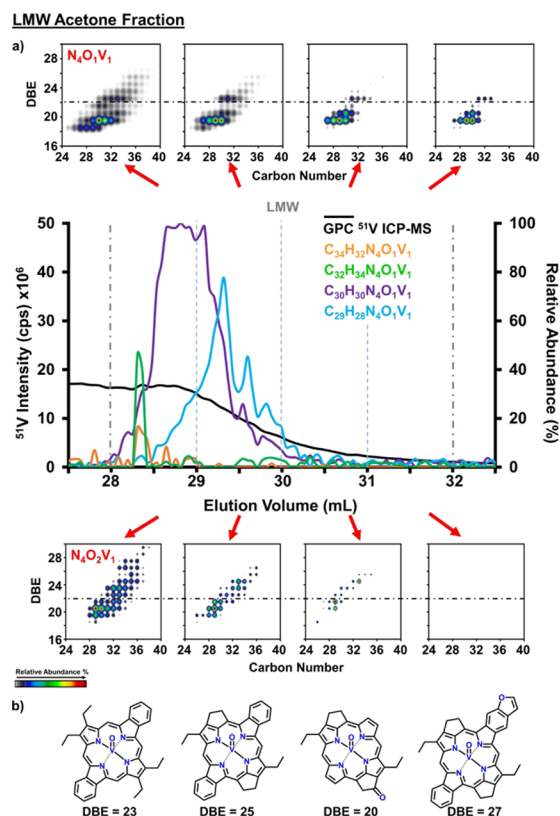
core, whereas Ni forms a square-planar complex; thus, vanadyl porphyrins elute earlier. Exocyclic rings are also correlated with less retention: the presence of a five-membered exocyclic ring decreases molecular planarity, precluding strong adsorption on the stationary phase.

Figure 5 presents the compositional range for the  $N_4O_1V_1$  class for the various GPC subfractions for the acetone and Tol/THF/MeOH PetroPhase 2017 extrography fractions. The Hep/Tol fraction is included in Supporting Information Figure S2. Figure 5 also shows the relative abundance of the most abundant vanadyl porphyrins as a function of elution volume. The acetone fraction reveals compositional trends similar to those of the whole asphaltene sample (Figure 4). Again, the most abundant species, detected as LMW aggregates (74 molecular formulas), reveal a narrower carbon number distribution than the MMW vanadyl porphyrins (134 molecular formulas). The results support the notion that sizable aggregates (MMW) are likely enriched with more alkyl-substituted compounds.

It is important to point out that in previous work, we reported the molecular composition of PetroPhase 2017 asphaltenes, accessed by direct-infusion (+) APPI FT-ICR MS. Vanadyl porphyrins were only observed in whole asphaltenes and the acetone fraction. However, in this work, Hep/Tol (Figure S2) and Tol/THF/MeOH fractions reveal abundant  $N_4O_1^{51}V_1$  compounds in the “monomeric” LMW region. We hypothesize that cooperative aggregation effects during direct-infusion MS analysis of complete extrography fractions prevent the detection of vanadyl porphyrins.<sup>29</sup> In this work, LMW Tol/THF/MeOH species reveal 27  $N_4O_1^{51}V_1$  formulas, and one prominent homologous series of 7 species (DBE 18) was detected in the MMW aggregates. The results confirm that separation by aggregate size distribution coupled to online FT-ICR MS detection, help to mitigate, to some extent, selective ionization.

Figure 6 presents the molecular composition for  $N_4O_1^{51}V_1$  and  $N_4O_2^{51}V_1$  classes of various elution ranges for the LMW region for the acetone fraction. The results indicate that the structural diversity narrows as a function of elution volume. Earlier-eluting  $N_4O_1^{51}V_1$  species (upper row, Figure 6a) exhibit up to ~38 carbon atoms and DBE ~26, which translates into a higher content of carbon atoms in alkyl-side chains (up to ~10) and more exocyclic rings. Possible structures are shown in Figure 6b, based on previous reports.<sup>57,83,95</sup> The last elution range (31–32 mL) only presents three prominent homologous series, and the majority of the detected species feature DBE = 19. The lower row of Figure 6a shows the compositional range of vanadyl porphyrins with an additional oxygen atom. The slightly higher DBE values, more evident for the first elution range (28–29 mL), suggest that oxygen may be incorporated as a ketone functionality or a furan ring (Figure 6b, right). In general, the content of side groups decreases for later-eluting compounds, which support the idea that exocyclic rings and alkyl-side chains hinder stronger interaction/longer residence on the GPC column. These results also agree with findings by Reynolds, Caumette, and Mironov *et al.*, who found that vanadyl porphyrins could elute late in the GPC separation of vacuum residues and asphaltenes.<sup>60,94,96–98</sup>

**Compositional Trends for Sulfur/Oxygen-Containing Heteroatomic Groups.** Figure 7, upper row, presents the GPC  $^{32}S$  ICP-MS chromatograms for acetone (left) and Tol/THF/MeOH (right) extrography fractions, along with the ICs (APPI FT-ICR MS) for selected S-containing heteroatomic



**Figure 6.** (a) DBE vs carbon number plots for  $N_4O_1^{51}V_1$  and  $N_4O_2^{51}V_1$  classes of various elution ranges for the LMW region for the acetone fraction; (b) suggested molecular structure for high DBE vanadyl porphyrins.

groups. For instance, the group  $S_x$  comprises  $S_1$ ,  $S_2$ ,  $S_3$ ,  $S_4$ , and  $S_5$  classes, and the group  $S_xO_y$  contains all the classes with both S and O atoms, such as  $S_1O_1$ ,  $S_1O_2$ ,  $S_1O_3$ ,  $S_2O_1$ , and  $S_2O_2$ , among others. The results indicate that  $^{32}S$ -containing compounds ( $S_x$ ,  $S_xO_y$ , and  $N_xO_yS_x$ ) follow trends similar to those for  $^{51}V$  species: MMW and LMW regions reveal the highest sulfur abundance in (+) APPI FT-ICR MS, whereas quantitative data (GPC  $^{32}S$  ICP-MS) points to much higher S amounts in the HMW aggregates, not effectively captured by MS detection. Table 2 includes the integrated areas for  $^{32}S$  (ICP-MS), which facilitate sample comparison.

Figure 7, lower row, presents combined DBE versus carbon number plots for S-containing heteroatomic groups for the various GPC subfractions. Abundance-weighted H/C ratios are included and assist data interpretation. The compositional trends indicate that sizable/medium aggregates, HMW and MMW, contain abundant alkyl-enriched compounds with H/C ratios much higher (up to  $H/C \sim 1.37$ ) than commonly reported values for asphaltene<sup>99,100</sup> and the LMW/tailing subfractions ( $H/C \sim 0.60$ – $0.89$ ). For both extrography fractions, HMW and MMW regions reveal longer homologous series, with up to ~40 carbon atoms in alkyl-side chains, and low-DBE (<15)  $S_xO_y$  compounds. Readers should keep into account that asphaltene are classically defined as highly aromatic species with an average of ~7 fused aromatic rings,<sup>3</sup> which translates into DBE values of 19–21.<sup>17,101</sup> We hypothesize that abundant oxygen-containing/polarizable functionalities, such as sulfoxides, rule the intermolecular forces responsible for the stronger aggregation of low-DBE/“atypical” compounds.<sup>74,102,103</sup> Furthermore, it is challenging

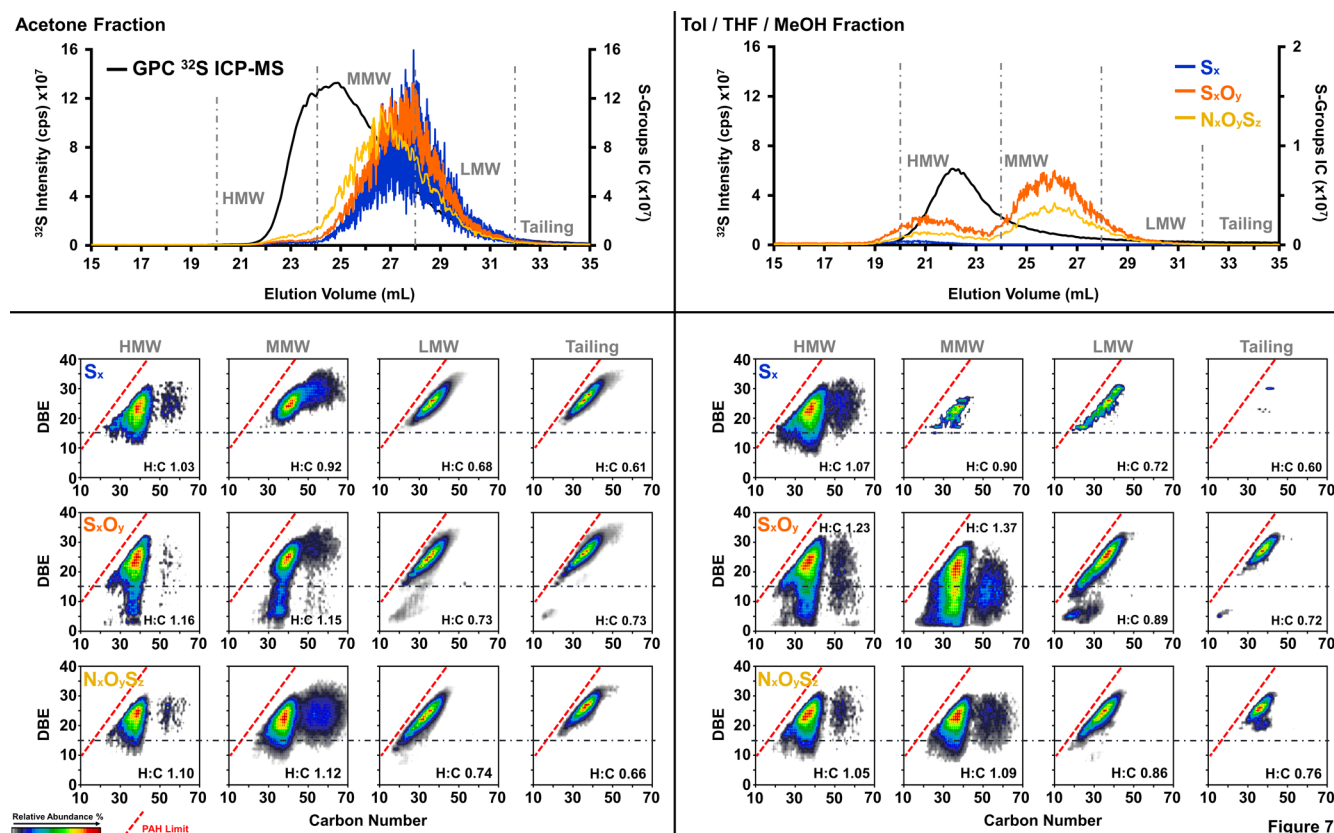


**Figure 7.** Upper row: GPC  $^{32}\text{S}$  ICP-MS and ICs for S-containing groups for acetone (left) and Tol/THF/MeOH (right). Lower row: DBE vs carbon number plots for  $\text{S}_x$ ,  $\text{S}_x\text{O}_y$ , and  $\text{N}_x\text{O}_y\text{S}_z$  groups. Abundance-weighted H/C ratios facilitate subfraction comparison.

**Table 2.** IAs (%) for the GPC  $^{32}\text{S}$  ICP-MS Chromatograms for Whole PetroPhase 2017 Asphaltenes and Its Acetone, Hep/Tol, and Tol/THF/MeOH Extrography Fractions

sample	prior to HMW <sup>a</sup> (%)	HMW (%)	MMW (%)	LMW (%)	tailing (%)
whole PetroPhase 2017 asphaltenes	1.11	64.64	25.52	6.12	2.61
acetone fraction	0.07	23.07	63.16	12.13	1.57
Hep/Tol fraction	3.09	65.78	20.70	5.86	4.57
Tol/THF/MeOH fraction	1.27	68.23	20.24	6.41	3.85

<sup>a</sup>Fraction eluted before the established molecular weight ranges. Material can elute before the defined MW ranges.

to establish the extent to which the detected heteroatom classes represent the real molecular composition of HMW/MMW aggregates. However, the abundance weighted H/C ratios suggest that the detected “atypical” species are likely abundant: their higher H/C ratios offset the substantial lower values of the LMW and tailing species.

The trends highlighted in Figure 7 are consistent with previous works by Putman *et al.*<sup>63,69</sup> who investigated the molecular composition of asphaltenes as a function of aggregate size and suggested that London forces between aliphatic moieties might be central in asphaltene self-assembly. In support of this hypothesis, for instance, Tanaka *et al.*<sup>104</sup> performed molecular dynamics simulations on model asphaltene compounds to understand the role of aliphatic chains and polar functionalities on the stability of aggregates upon heating. Simulations for structures in which aliphatic side chains were removed and heteroatoms were replaced with

carbon revealed that dissociation occurred at much lower temperatures. The authors also pointed out that coal molecules are comprised of smaller aromatic cores and fewer aliphatic carbons, whereas asphaltenes reveal higher content of longer alkyl side chains attached to bigger aromatic cores. Therefore, differences in solubility in common solvents for coal and asphaltenes should be ruled by alkyl-chain and heteroatom content, and thus, it seems plausible that aliphatic side chains and polar groups can affect the aggregate stability. The authors concluded that removal of alkyl side chains caused a decrease in the interaction energy, likely, in part, because of lack of London forces between aliphatic side chains, which decreased the stability of the aggregated structures. Furthermore, entanglement of long aliphatic chains was also suggested to stabilize the aggregates. Supporting Information, Figure S3, includes the DBE versus carbon number plots for S-containing groups for the GPC subfractions from whole PetroPhase 2017 asphaltenes and its Hep/Tol extrography fraction, which exhibit DBE and carbon number tendencies consistent with acetone and Tol/THF/MeOH.

All the samples feature an interesting trend for the PAH limit, which is highlighted by the red dashed line in the DBE versus carbon number plots of Figure 7 and is defined as the highest possible DBE value, at a given carbon number, for fossil hydrocarbons with a planar molecular structure. The PAH limit is determined by eq 2<sup>105–107</sup> and dictates that the DBE of planar hydrocarbons do not exceed the ~90% of its carbon number. Species close to the PAH limit, to the right, are highly aromatic/pericondensed; molecular formulas with DBE values above the limit are inherent to fullerene-like structures. Figures 7 and S3 indicate that the compositional

range moves toward the PAH limit as a function of elution volume, suggesting that weakly-aggregated/monomeric species contain abundant highly aromatic/pericondensed “classical” asphaltenes.

$$\text{DBE} = 0.899 \times \text{carbon number} \quad (2)$$

Figure 8, upper row, presents the compositional range of S-containing groups for the complete acetone extrography

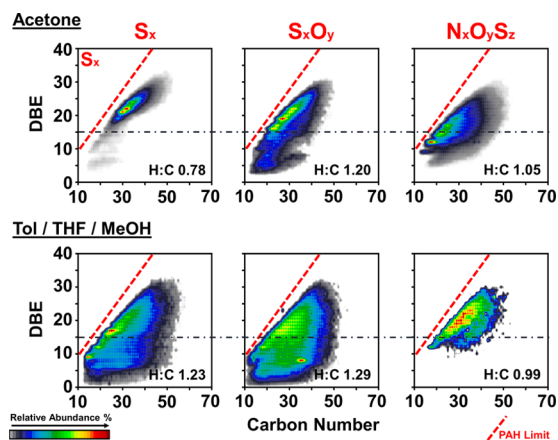


**Figure 8.** Compositional range for S-containing heteroatom groups accessed by direct infusion (+) APPI FT-ICR MS for complete acetone (upper row) and Tol/THF/MeOH (lower row) fractions extrography fractions.

fraction, derived from direct-infusion (+) APPI FT-ICR MS characterization.<sup>29</sup> The results confirm the preferential access to highly-aromatic/hydrogen-deficient  $S_x$  compounds, similar to the species observed in the LMW and tailing GPC subfractions, which comprise only  $\sim 14\%$  of the total sulfur content (GPC  $^{32}\text{S}$  ICP–MS, Table 2). Furthermore, direct infusion MS hints some of the  $S_xO_y$  and  $N_xO_yS_z$  species that feature a higher content of carbon atoms in alkyl-side chains and slightly lower DBE values, detected in the MMW GPC region ( $\sim 63\%$  sulfur content). Figure 8, lower row, presents the composition of the complete Tol/THF/MeOH extrography fraction and reveals low-DBE  $S_x$  and  $S_xO_y$  compounds with H/C ratios somehow similar to those observed in HMW/MMW GPC regions ( $\sim 88\%$  sulfur content). Collectively, the results indicate that the species revealed by direct infusion MS are determined by both ionization efficiency (MIY) and actual concentration. LMW/tailing Tol/THF/MeOH S-containing compounds, although they ionize more efficiently, are in minimal abundance and thus do not dominate the compositional range revealed by direct infusion MS.

**Implications for Novel Aggregation Models for Petroleum Asphaltenes.** The online GPC ICP–MS ( $V^{51}$ ) analysis of the whole PetroPhase 2017 asphaltene and its extrography fractions confirmed the success of the fractionation procedure in the isolation of fractions with varying degrees of aggregation. Specifically, the acetone extrography fraction was the most unaggregated fraction and comprised most of the MMW/LMW  $V^{51}$  containing species. Conversely, the Hep/Tol and Tol/THF/MeOH extrography fractions were shifted to lower elution volumes and resided in the HMW (large aggregate size) region of the GPC chromatogram. Comparison of the quantitative GPC ICR–MS ( $V^{51}$ ) to that of an identical GPC separation coupled online to a 21 T FT-ICR mass spectrometer revealed several trends that support prior offline

observations: (1) despite high  $V^{51}$  ICP–MS concentrations in the HMW region, very few vanadyl porphyrins were detected by MS. (2) The vanadyl porphyrins detected by MS in the HMW region of the GPC chromatogram were of the lowest carbon number and similar to those detected in the LMW/tailing fraction. (3) Vanadyl porphyrins had the widest carbon number ranges at the end of the MMW/beginning of the LMW region and progressively dropped in carbon number with elution volume (from end of MMW to the final tailing fraction). (4) The MIY of the HMW fraction was more than  $\sim 10$ -fold lower than that of the medium and LMW regions despite 2-fold higher  $V^{51}$  concentrations. (5) The overlap in measure  $V^{51}$  concentrations and TIC (by MS) for vanadyl porphyrins was greatest for the LMW region of the GPC chromatogram. (6) Similar experiments monitoring  $S^{32}$  revealed a greater overlap between the ICP and FT-ICR MS results in the MMW region compared to vanadyl porphyrins and exposed sulfur-containing species that are not detected in offline analysis of the GPC fractions. (7) The offline MS analysis of the GPC fractions most closely resembles that of the LMW/tailing fraction. Collectively, the results support prior observations that aggregation is most likely responsible for the extremely low MIY in the APPI MS analysis of high and MMW regions of the GPC chromatogram. Simply, these species appear to exist as stable aggregates, and thus the amount of unaggregated material available for ionization/detection in the  $200 < m/z < 2000$  range is very low. Whether the aggregates are ionized and available for detection at much higher  $m/z$  values is not known.<sup>108</sup> The most striking result is the comparison of the vanadyl porphyrins to the sulfur species detected in the HMW/MMW regions. The vanadyl porphyrins are at their lowest carbon numbers in these fractions (close to the PAH limit), whereas the sulfur species are displaced from the PAH line with their widest carbon number and DBE ranges. The vanadyl porphyrins reach their greatest width in carbon number ranges at the end of the medium/beginning of the LMW region but progressively compress their carbon number range as elution progresses through the LMW and into the tailing fraction. Sulfur-containing species exhibit similar behavior and end closest to the PAH line in the tailing fractions. Given that previous tandem MS experiments have demonstrated the island fragmentation behavior of the PetroPhase 2017 asphaltene acetone fraction and archipelago fragmentation of the Hep/Tol and Tol/THF/MeOH fractions, the same MIY trends as a function of extrography fraction (acetone, high MIY and Tol/THF/MeOH, lowest MIY), and revealed that the stability trend for heptane titration of a toluene solution of extrography fractions is acetone (most stable), Hep/Tol (less stable), to Tol/THF/MeOH (least stable); the results presented herein strongly suggest that the archipelago dominant Hep/Tol and Tol/THF/MeOH extrography fractions of the PetroPhase 2017 asphaltenes are strongly aggregated and a large fraction of the vanadyl porphyrin species remain locked inside the aggregate and are thus unavailable for ionization/detection by MS. Those porphyrins that are available are alkyl deficient and most likely absorbed to the aggregate surface. Unaggregated porphyrins are readily detected in the LMW/tailing fractions and elute from higher alkylated to lower alkylated species as previously observed with other GPC/FT-ICR MS studies. Conversely, sulfur-containing species are most highly alkylated in the HMW/MMW regions and compress quickly in their carbon number distribution widths in the LMW/tailing fraction. If one assumes that this

contradictory behavior between the observed vanadyl porphyrins and sulfur-containing species is attributable to species that are absorbed on the aggregate surface (vanadyl porphyrins) to some fraction of those present in the aggregate (sulfur species), the large differences in the widths of their corresponding carbon number distribution ( $\sim 5$  for vanadyl porphyrins compared to  $\sim 40$  for sulfur-containing species) supports the importance of London forces between alkane moieties in stable aggregates.

## CONCLUDING REMARKS

The interlaboratory sample known as PetroPhase 2017 asphaltene and its extrography fractions were separated via GPC into four fractions: HMW (aggregates), MMW, LMW (non-aggregated/monomers), and “tailing” (free species). The separation was hyphenated to elemental analysis by  $^{51}\text{V}/^{32}\text{S}$ -ICP-MS (quantitative) and APPI 21 T-FT-ICR-MS (molecular formula assignment).

Quantitative results via ICP-MS and compositional features accessed by FT-ICR MS indicate:

- Extrography yields asphaltene fractions with distinctive aggregation behavior. Acetone reveals abundant MMW and LMW species, whereas Hep/Tol and Tol/THF/MeOH are enriched with highly aggregated compounds (HMW).
- Ion production (as detected by APPI FT-ICR MS) is inversely proportional to aggregate size (determined by GPC). The acetone fraction, shown to aggregate to a lesser extent than Tol/THF/MeOH, reveals the highest production efficiency of non-aggregated V/S-containing compounds.
- ICs for specific molecular formulas, mostly detected in the monomeric GPC fractions, suggest that alkyl-chain content and exocyclic rings govern the elution behavior of free/non-aggregated porphyrins. “Free”/highly substituted vanadyl porphyrins elute earlier likely because of their decreased interaction with the GPC column.
- Compositional trends for S-containing molecules indicate that HMW/MMW aggregates contain abundant species with a higher content of carbon atoms in alkyl-side chains. For these GPC fractions, oxygen-rich compounds ( $\text{SO}_x$  classes) feature low DBE values. Conversely, non-aggregated/monomeric GPC fractions (LMW/tailing) reveal abundant highly aromatic, likely percondensed, alkyl-depleted molecules.
- These structural features suggest that alkyl-side chain moieties and polarizable functionalities could have a central role in asphaltene aggregation. In other words,  $\pi$ -stacking is not the dominant intermolecular force that rules petroleum aggregation.
- The results indicate that APPI MS characterization is highly limited by aggregation, and advanced separations, as well as online FT-ICR MS detection, are required to overcome these limitations.

## ASSOCIATED CONTENT

### Supporting Information

The Supporting Information is available free of charge at <https://pubs.acs.org/doi/10.1021/acs.energyfuels.0c03349>.

MIY and  $^{51}\text{V}$  GPC ICP-MS chromatogram for whole PetroPhase 2017 asphaltene; compositional range for vanadyl porphyrins for all GPC subfractions and ICs for

selected  $\text{N}_4\text{O}_1^{51}\text{V}_1$  molecular formulas for Hep/Tol PetroPhase 2017 asphaltene; GPC  $^{32}\text{S}$  ICP-MS and ICs for S-containing groups for whole PetroPhase 2017 asphaltene and its Hep/Tol fraction; and DBE versus carbon number plots for  $\text{S}_x$ ,  $\text{S}_x\text{O}_y$ , and  $\text{N}_x\text{O}_y\text{S}_z$  groups (PDF)

## AUTHOR INFORMATION

### Corresponding Authors

**Brice Bouyssiere** – International Joint Laboratory iC2MC: Complex Matrices Molecular Characterization, Total Research & Technology, Gonfreville, 76700 Harfleur, France; Université de Pau et des Pays de l'Adour, E2S UPPA, CNRS, IPREM, Institut des Sciences Analytiques et de Physico-chimie pour l'Environnement et les Matériaux, UMR5254, Hélioparc, 64053 Pau, France; [orcid.org/0000-0001-5878-6067](https://orcid.org/0000-0001-5878-6067); Email: [brice.bouyssiere@univ-pau.fr](mailto:brice.bouyssiere@univ-pau.fr)

**Ryan P. Rodgers** – Ion Cyclotron Resonance Program, National High Magnetic Field Laboratory and Future Fuels Institute, Florida State University, Tallahassee, Florida 32310, United States; International Joint Laboratory iC2MC: Complex Matrices Molecular Characterization, Total Research & Technology, Gonfreville, 76700 Harfleur, France; Université de Pau et des Pays de l'Adour, E2S UPPA, CNRS, IPREM, Institut des Sciences Analytiques et de Physico-chimie pour l'Environnement et les Matériaux, UMR5254, Hélioparc, 64053 Pau, France; [orcid.org/0000-0003-1302-2850](https://orcid.org/0000-0003-1302-2850); Email: [rodders@magnet.fsu.edu](mailto:rodders@magnet.fsu.edu)

### Authors

**Martha L. Chacón-Patiño** – Ion Cyclotron Resonance Program, National High Magnetic Field Laboratory, Florida State University, Tallahassee, Florida 32310, United States; International Joint Laboratory iC2MC: Complex Matrices Molecular Characterization, Total Research & Technology, Gonfreville, 76700 Harfleur, France; [orcid.org/0000-0002-7273-5343](https://orcid.org/0000-0002-7273-5343)

**Rémi Mouliau** – International Joint Laboratory iC2MC: Complex Matrices Molecular Characterization, Total Research & Technology, Gonfreville, 76700 Harfleur, France; Université de Pau et des Pays de l'Adour, E2S UPPA, CNRS, IPREM, Institut des Sciences Analytiques et de Physico-chimie pour l'Environnement et les Matériaux, UMR5254, Hélioparc, 64053 Pau, France

**Caroline Barrère-Mangote** – International Joint Laboratory iC2MC: Complex Matrices Molecular Characterization, Total Research & Technology, Gonfreville, 76700 Harfleur, France; TOTAL Raffinage Chimie, TRTG, 76700 Harfleur, France

**Jonathan C. Putman** – Ion Cyclotron Resonance Program, National High Magnetic Field Laboratory, Florida State University, Tallahassee, Florida 32310, United States

**Chad R. Weisbrod** – Ion Cyclotron Resonance Program, National High Magnetic Field Laboratory, Florida State University, Tallahassee, Florida 32310, United States; [orcid.org/0000-0001-5324-4525](https://orcid.org/0000-0001-5324-4525)

**Greg T. Blakney** – Ion Cyclotron Resonance Program, National High Magnetic Field Laboratory, Florida State University, Tallahassee, Florida 32310, United States; [orcid.org/0000-0002-4205-9866](https://orcid.org/0000-0002-4205-9866)

**Pierre Giusti** – International Joint Laboratory iC2MC: Complex Matrices Molecular Characterization, Total Research & Technology, Gonfreville, 76700 Harfleur, France;

TOTAL Raffinage Chimie, TRTG, 76700 Harfleur, France;  
orcid.org/0000-0002-9569-3158

Complete contact information is available at:  
<https://pubs.acs.org/10.1021/acs.energyfuels.0c03349>

## Notes

The authors declare no competing financial interest.

## ACKNOWLEDGMENTS

A portion of this work was performed at the National High Magnetic Field Laboratory ICR User Facility, which is supported by the National Science Foundation Division of Chemistry through Cooperative Agreements DMR-1157490 and DMR-1644779, and the State of Florida; and Conseil Régional d'Aquitaine (20071303002PFM), and FEDER (31486/08011464). The authors thank TOTAL and Professor Marianny Combariza, Industrial University of Santander–Colombia, for supplying the PetroPhase 2017 asphaltenes.

## REFERENCES

- (1) Molnár, G. L.; Schrader, W. New Separation Approach for Asphaltene Investigation: Argentation Chromatography Coupled with Ultrahigh-Resolution Mass Spectrometry. *Energy Fuels* **2015**, *29*, 6224–6230.
- (2) Moir, M. E. *Asphaltene, What Art Thou?: Asphaltene and the Boduszynski Continuum*; ACS Symposium Series; American Chemical Society, 2018.
- (3) Mullins, O. C. The Modified Yen Model. *Energy Fuels* **2010**, *24*, 2179–2207.
- (4) Gray, M. R. Whatsoever things are true: Hypothesis, artefact, and bias in chemical engineering research. *Can. J. Chem. Eng.* **2020**, *1–14*.
- (5) Schuler, B.; Meyer, G.; Peña, D.; Mullins, O. C.; Gross, L. Unraveling the Molecular Structures of Asphaltene by Atomic Force Microscopy. *J. Am. Chem. Soc.* **2015**, *137*, 9870–9876.
- (6) Schuler, B.; Fatayer, S.; Meyer, G.; Rogel, E.; Moir, M.; Zhang, Y.; Harper, M. R.; Pomerantz, A. E.; Bake, K. D.; Witt, M.; et al. Heavy Oil Based Mixtures of Different Origins and Treatments Studied by Atomic Force Microscopy. *Energy Fuels* **2017**, *31*, 6856–6861.
- (7) Kaiser, N. K.; Quinn, J. P.; Blakney, G. T.; Hendrickson, C. L.; Marshall, A. G. A Novel 9.4 Tesla FTICR Mass Spectrometer with Improved Sensitivity, Mass Resolution, and Mass Range. *J. Am. Soc. Mass Spectrom.* **2011**, *22*, 1343–1351.
- (8) Hendrickson, C. L.; Quinn, J. P.; Kaiser, N. K.; Smith, D. F.; Blakney, G. T.; Chen, T.; Marshall, A. G.; Weisbrod, C. R.; Beu, S. C. 21 Tesla Fourier Transform Ion Cyclotron Resonance Mass Spectrometer: A National Resource for Ultrahigh Resolution Mass Analysis. *J. Am. Soc. Mass Spectrom.* **2015**, *26*, 1626–1632.
- (9) Niles, S. F.; Chacón-Patiño, M. L.; Smith, D. F.; Rodgers, R. P.; Marshall, A. G. Comprehensive Compositional and Structural Comparison of Coal and Petroleum Asphaltene Based on Extrography Fractionation Coupled with Fourier Transform Ion Cyclotron Resonance MS and MS/MS Analysis. *Energy Fuels* **2020**, *34*, 1492–1505.
- (10) Mullins, O. C.; Sabbah, H.; Eyssautier, J.; Pomerantz, A. E.; Barré, L.; Andrews, A. B.; Ruiz-Morales, Y.; Mostowfi, F.; McFarlane, R.; Goual, L.; Lepkowitz, R.; Cooper, T.; Orbulescu, J.; Leblanc, R. M.; Edwards, J.; Zare, R. N. Advances in Asphaltene Science and the Yen–Mullins Model. *Energy Fuels* **2012**, *26*, 3986–4003.
- (11) Mullins, O. C. The Asphaltene. *Annu. Rev. Anal. Chem.* **2011**, *4*, 393–418.
- (12) Barré, L.; Espinat, D.; Rosenberg, E.; Scarsella, M. Colloidal Structure of Heavy Crudes and Asphaltene Solutions. *Rev. Inst. Fr. Pét.* **1997**, *52*, 161–175.
- (13) Chen, P.; Joshi, Y. V.; Metz, J. N.; Yao, N.; Zhang, Y. Conformational Analysis of Nonplanar Archipelago Structures on a Cu (111) Surface by Molecular Imaging. *Energy Fuels* **2020**, *34*, 12135–12141.
- (14) Schuler, B.; Zhang, Y.; Liu, F.; Pomerantz, A. E.; Andrews, A. B.; Gross, L.; Pauchard, V.; Banerjee, S.; Mullins, O. C. Overview of Asphaltene Nanostructures and Thermodynamic Applications. *Energy Fuels* **2020**, DOI: 10.1021/acs.energyfuels.0c00874.
- (15) Zuo, J. Y.; Jackson, R.; Agarwal, A.; Herold, B.; Kumar, S.; De Santo, I.; Dumont, H.; Ayan, C.; Beardsell, M.; Mullins, O. C. Diffusion Model Coupled with the Flory-Huggins-Zuo Equation of State and Yen-Mullins Model Accounts for Large Viscosity and Asphaltene Variations in a Reservoir Undergoing Active Biodegradation. *Energy Fuels* **2015**, *29*, 1447–1460.
- (16) Chacón-Patiño, M. L.; Rowland, S. M.; Rodgers, R. P. Advances in Asphaltene Petroleomics. Part 1: Asphaltene Are Composed of Abundant Island and Archipelago Structural Motifs. *Energy Fuels* **2017**, *31*, 13509–13518.
- (17) Podgorski, D. C.; Corilo, Y. E.; Nyadong, L.; Lobodin, V. V.; Bythell, B. J.; Robbins, W. K.; McKenna, A. M.; Marshall, A. G.; Rodgers, R. P. Heavy Petroleum Composition. 5. Compositional and Structural Continuum of Petroleum Revealed. *Energy Fuels* **2013**, *27*, 1268–1276.
- (18) Savage, P. E.; Klein, M. T.; Kukes, S. G. Asphaltene Reaction Pathways. 1. Thermolysis. *Ind. Eng. Chem. Process Des. Dev.* **1985**, *24*, 1169–1174.
- (19) Karimi, A.; Qian, K.; Olmstead, W. N.; Freund, H.; Yung, C.; Gray, M. R. Quantitative Evidence for Bridged Structures in Asphaltene by Thin Film Pyrolysis. *Energy Fuels* **2011**, *25*, 3581–3589.
- (20) Rueda-Velásquez, R. I.; Freund, H.; Qian, K.; Olmstead, W. N.; Gray, M. R. Characterization of Asphaltene Building Blocks by Cracking under Favorable Hydrogenation Conditions. *Energy Fuels* **2013**, *27*, 1817–1829.
- (21) Gray, M. R.; Tykwinski, R. R.; Stryker, J. M.; Tan, X. Supramolecular Assembly Model for Aggregation of Petroleum Asphaltene. *Energy Fuels* **2011**, *25*, 3125–3134.
- (22) Castillo, J.; Vargas, V. Metal Porphyrin Occlusion: Adsorption during Asphaltene Aggregation. *Pet. Sci. Technol.* **2016**, *34*, 873–879.
- (23) Qiao, P.; Harbottle, D.; Tchoukov, P.; Masliyah, J.; Sjöblom, J.; Liu, Q.; Xu, Z. Fractionation of Asphaltene in Understanding Their Role in Petroleum Emulsion Stability and Fouling. *Energy Fuels* **2017**, *31*, 3330–3337.
- (24) Yang, F.; Tchoukov, P.; Dettman, H.; Teklebrhan, R. B.; Liu, L.; Dabros, T.; Czarnecki, J.; Masliyah, J.; Xu, Z. Asphaltene Subfractions Responsible for Stabilizing Water-in-Crude Oil Emulsions. Part 2: Molecular Representations and Molecular Dynamics Simulations. *Energy Fuels* **2015**, *29*, 4783–4794.
- (25) Natarajan, A.; Kuznicki, N.; Harbottle, D.; Masliyah, J.; Zeng, H.; Xu, Z. Understanding Mechanisms of Asphaltene Adsorption from Organic Solvent on Mica. *Langmuir* **2014**, *30*, 9370–9377.
- (26) Hsu, C. S.; Hendrickson, C. L.; Rodgers, R. P.; McKenna, A. M.; Marshall, A. G. Petroleomics: Advanced Molecular Probe for Petroleum Heavy Ends. *J. Mass Spectrom.* **2011**, *46*, 337–343.
- (27) Rodgers, R. P.; Marshall, A. G. Petroleomics: Advanced Characterization of Petroleum-Derived Materials by Fourier Transform Ion Cyclotron Resonance Mass Spectrometry (FT-ICR MS). In *Asphaltene, Heavy Oils, and Petroleomics*; Mullins, O. C., Sheu, E. Y., Hammam, A., Marshall, A. G., Eds.; Springer, 2007; pp 63–93.
- (28) McKenna, A. M.; Williams, J. T.; Putman, J. C.; Aeppli, C.; Reddy, C. M.; Valentine, D. L.; Lemkau, K. L.; Kellermann, M. Y.; Savory, J. J.; Kaiser, N. K.; et al. Unprecedented Ultrahigh Resolution FT-ICR Mass Spectrometry and Parts-per-Billion Mass Accuracy Enable Direct Characterization of Nickel and Vanadyl Porphyrins in Petroleum from Natural Seeps. *Energy Fuels* **2014**, *28*, 2454–2464.
- (29) Chacón-Patiño, M. L.; Rowland, S. M.; Rodgers, R. P. Advances in Asphaltene Petroleomics. Part 2: Selective Separation Method That Reveals Fractions Enriched in Island and Archipelago Structural Motifs by Mass Spectrometry. *Energy Fuels* **2018**, *32*, 314–328.

- (30) Chacón-Patiño, M. L.; Rowland, S. M.; Rodgers, R. P. Advances in Asphaltene Petroleomics. Part 3. Dominance of Island or Archipelago Structural Motif Is Sample Dependent. *Energy Fuels* **2018**, *32*, 9106–9120.
- (31) Wittrig, A. M.; Fredriksen, T. R.; Qian, K.; Clingenpeel, A. C.; Harper, M. R. Single Dalton Collision-Induced Dissociation for Petroleum Structure Characterization. *Energy Fuels* **2017**, *31*, 13338–13344.
- (32) Rüger, C. P.; Miersch, T.; Schwemer, T.; Sklorz, M.; Zimmermann, R. Hyphenation of Thermal Analysis to Ultrahigh-Resolution Mass Spectrometry (Fourier Transform Ion Cyclotron Resonance Mass Spectrometry) Using Atmospheric Pressure Chemical Ionization For Studying Composition and Thermal Degradation of Complex Materials. *Anal. Chem.* **2015**, *87*, 6493–6499.
- (33) Rüger, C. P.; Grimmer, C.; Sklorz, M.; Neumann, A.; Streibel, T.; Zimmermann, R. Combination of Different Thermal Analysis Methods Coupled to Mass Spectrometry for the Analysis of Asphaltenes and Their Parent Crude Oils: Comprehensive Characterization of the Molecular Pyrolysis Pattern. *Energy Fuels* **2017**, *32*, 2699–2711.
- (34) Rüger, C. P.; Neumann, A.; Sklorz, M.; Schwemer, T.; Zimmermann, R. Thermal Analysis Coupled to Ultrahigh Resolution Mass Spectrometry with Collision Induced Dissociation for Complex Petroleum Samples: Heavy Oil Composition and Asphaltene Precipitation Effects. *Energy Fuels* **2017**, *31*, 13144–13158.
- (35) Nyadong, L.; Lai, J.; Thompson, C.; LaFrancois, C. J.; Cai, X.; Song, C.; Wang, J.; Wang, W. High-Field Orbitrap Mass Spectrometry and Tandem Mass Spectrometry for Molecular Characterization of Asphaltenes. *Energy Fuels* **2018**, *32*, 294–305.
- (36) Dong, X.; Zhang, Y.; Milton, J.; Yerabolu, R.; Easterling, L.; Kenttämaa, H. I. Investigation of the relative abundances of single-core and multicore compounds in asphaltenes by using high-resolution in-source collision-activated dissociation and medium-energy collision-activated dissociation mass spectrometry with statistical considerations. *Fuel* **2019**, *246*, 126–132.
- (37) Qiao, P.; Harbottle, D.; Li, Z.; Tang, Y.; Xu, Z. Interactions of Asphaltene Subfractions in Organic Media of Varying Aromaticity. *Energy Fuels* **2018**, *32*, 10478.
- (38) Ballard, D. A.; Chacón-Patiño, M. L.; Qiao, P.; Roberts, K. J.; Rae, R.; Dowding, P. J.; Xu, Z.; Harbottle, D. Molecular Characterization of Strongly- and Weakly-Interfacially Active Asphaltenes by High-Resolution Mass Spectrometry. *Energy Fuels* **2020**, *34*, 13966.
- (39) Clingenpeel, A. C.; Rowland, S. M.; Corilo, Y. E.; Zito, P.; Rodgers, R. P. Fractionation of Interfacial Material Reveals a Continuum of Acidic Species That Contribute to Stable Emulsion Formation. *Energy Fuels* **2017**, *31*, 5933–5939.
- (40) Jarvis, J. M.; Robbins, W. K.; Corilo, Y. E.; Rodgers, R. P. Novel Method to Isolate Interfacial Material. *Energy Fuels* **2015**, *29*, 7058–7064.
- (41) Boduszynski, M. M. Composition of Heavy Petroleum. 1. Molecular Weight, Hydrogen Deficiency, and Heteroatom Concentration as a Function of Atmospheric Equivalent Boiling Point up to 1400 °F (760 °C). *Energy Fuels* **1987**, *1*, 2–11.
- (42) McKenna, A. M.; Purcell, J. M.; Rodgers, R. P.; Marshall, A. G. Heavy Petroleum Composition. 1. Exhaustive Compositional Analysis of Athabasca Bitumen HVGO Distillates by Fourier Transform Ion Cyclotron Resonance Mass Spectrometry: A Definitive Test of the Boduszynski Model. *Energy Fuels* **2010**, *24*, 2929–2938.
- (43) McKenna, A. M.; Blakney, G. T.; Xian, F.; Glaser, P. B.; Rodgers, R. P.; Marshall, A. G. Heavy Petroleum Composition. 2. Progression of the Boduszynski Model to the Limit of Distillation by Ultrahigh-Resolution FT-ICR Mass Spectrometry. *Energy Fuels* **2010**, *24*, 2939–2946.
- (44) Chacón-Patiño, M. L.; Rowland, S. M.; Rodgers, R. P. The Compositional and Structural Continuum of Petroleum from Light Distillates to Asphaltenes: The Boduszynski Continuum Theory As Revealed by FT-ICR Mass Spectrometry. In *The Boduszynski Continuum: Contributions to the Understanding of the Molecular Composition of Petroleum*; Ovalles, C., Moir, M. E., Eds.; ACS Symposium Series; American Chemical Society: Washington, DC, 2018; Vol. 1282, pp 113–171.
- (45) Rodgers, R. P.; Schaub, T. M.; Marshall, A. G. Petroleomics: MS Returns to Its Roots. *Anal. Chem.* **2005**, *77*, 20 A–27 A.
- (46) Qian, K.; Edwards, K. E.; Diehl, J. H.; Green, L. A. Fundamentals and Applications of Electrospray Ionization Mass Spectrometry for Petroleum Characterization. *Energy Fuels* **2004**, *18*, 1784–1791.
- (47) Purcell, J. M.; Hendrickson, C. L.; Rodgers, R. P.; Marshall, A. G. Atmospheric Pressure Photoionization Proton Transfer for Complex Organic Mixtures Investigated by Fourier Transform Ion Cyclotron Resonance Mass Spectrometry. *J. Am. Soc. Mass Spectrom.* **2007**, *18*, 1682–1689.
- (48) Ramírez-Pradilla, J. S.; Blanco-Tirado, C.; Hubert-Roux, M.; Giusti, P.; Afonso, C.; Combariza, M. Y. Comprehensive Petroporphyrin Identification in Crude Oils Using Highly Selective Electron Transfer Reactions in MALDI-FTICR-MS. *Energy Fuels* **2019**, *33*, 3899–3907.
- (49) Gaspar, A.; Zellermann, E.; Lababidi, S.; Reece, J.; Schrader, W. Characterization of Saturates, Aromatics, Resins, and Asphaltenes Heavy Crude Oil Fractions by Atmospheric Pressure Laser Ionization Fourier Transform Ion Cyclotron Resonance Mass Spectrometry. *Energy Fuels* **2012**, *26*, 3481–3487.
- (50) Gaspar, A.; Zellermann, E.; Lababidi, S.; Reece, J.; Schrader, W. Impact of Different Ionization Methods on the Molecular Assignments of Asphaltenes by FT-ICR Mass Spectrometry. *Anal. Chem.* **2012**, *84*, 5257–5267.
- (51) Pomerantz, A. E.; Hammond, M. R.; Morrow, A. L.; Mullins, O. C.; Zare, R. N. Two-Step Laser Mass Spectrometry of Asphaltenes. *J. Am. Chem. Soc.* **2008**, *130*, 7216–7217.
- (52) Gutiérrez Sama, S.; Farenc, M.; Barrère-Mangote, C.; Lobinski, R.; Afonso, C.; Bouyssièrè, B.; Giusti, P. Molecular Fingerprints and Speciation of Crude Oils and Heavy Fractions Revealed by Molecular and Elemental Mass Spectrometry: Keystone between Petroleomics, Metallopetroleomics, and Petrointeractomics. *Energy Fuels* **2018**, *32*, 4593–4605.
- (53) Farenc, M.; Corilo, Y. E.; Lalli, P. M.; Riches, E.; Rodgers, R. P.; Afonso, C.; Giusti, P. Comparison of Atmospheric Pressure Ionization for the Analysis of Heavy Petroleum Fractions with Ion Mobility-Mass Spectrometry. *Energy Fuels* **2016**, *30*, 8896–8903.
- (54) Huba, A. K.; Huba, K.; Gardinali, P. R. Understanding the Atmospheric Pressure Ionization of Petroleum Components: The Effects of Size, Structure, and Presence of Heteroatoms. *Sci. Total Environ.* **2016**, *568*, 1018–1025.
- (55) Cho, Y.; Na, J.-G.; Nho, N.-S.; Kim, S.; Kim, S. Application of Saturates, Aromatics, Resins, Asphaltenes Crude Oil Fractionation for Detailed Chemical Characterization of Heavy Crude Oils by Fourier Transform Ion Cyclotron Resonance Mass Spectrometry Equipped with Atmospheric Pressure Photoionization. *Energy Fuels* **2012**, *26*, 2558–2565.
- (56) Buenrostro-Gonzalez, E.; Andersen, S. I.; Garcia-Martinez, J. A.; Lira-Galeana, C. Solubility/Molecular Structure Relationships of Asphaltenes in Polar and Nonpolar Media. *Energy Fuels* **2002**, *16*, 732–741.
- (57) Zhang, Y.; Schulz, F.; Rytting, B. M.; Walters, C. C.; Kaiser, K.; Metz, J. N.; Harper, M. R.; Merchant, S. S.; Mennito, A. S.; Qian, K.; et al. Elucidating the Geometric Substitution of Petroporphyrins by Spectroscopic Analysis and Atomic Force Microscopy Molecular Imaging. *Energy Fuels* **2019**, *33*, 6088–6097.
- (58) Gutierrez Sama, S.; Desprez, A.; Krier, G.; Lienemann, C. P.; Barbier, J.; Lobinski, R.; Barrère-Mangote, C.; Giusti, P.; Bouyssièrè, B. Study of the Aggregation of Metal Complexes with Asphaltenes Using Gel Permeation Chromatography Inductively Coupled Plasma High-Resolution Mass Spectrometry. *Energy Fuels* **2016**, *30*, 6907–6912.
- (59) Ligiero, L. M.; Bouriat, P.; Dicharry, C.; Passade-Boupat, N.; Lalli, P. M.; Rodgers, R. P.; Barrère-Mangote, C.; Giusti, P.; Bouyssièrè, B. Characterization of Crude Oil Interfacial Material

Isolated by the Wet Silica Method. Part 1: Gel Permeation Chromatography Inductively Coupled Plasma High-Resolution Mass Spectrometry Analysis. *Energy Fuels* **2017**, *31*, 1065–1071.

(60) Caumette, G.; Lienemann, C.-P.; Merdrignac, I.; Bouyssiere, B.; Lobinski, R. Fractionation and Speciation of Nickel and Vanadium in Crude Oils by Size Exclusion Chromatography-ICP MS and Normal Phase HPLC-ICP MS. *J. Anal. At. Spectrom.* **2010**, *25*, 1123–1129.

(61) Desprez, A.; Bouyssiere, B.; Arnaudguilhem, C.; Krier, G.; Vernex-Loset, L.; Giusti, P. Study of the Size Distribution of Sulfur, Vanadium, and Nickel Compounds in Four Crude Oils and Their Distillation Cuts by Gel Permeation Chromatography Inductively Coupled Plasma High-Resolution Mass Spectrometry. *Energy Fuels* **2014**, *28*, 3730–3737.

(62) Berruoco, C.; Venditti, S.; Morgan, T. J.; Álvarez, P.; Millan, M.; Herod, A. A.; Kandiyoti, R. Calibration of Size-Exclusion Chromatography Columns with 1-Methyl-2-Pyrrolidinone (NMP)/Chloroform Mixtures as Eluent: Applications to Petroleum-Derived Samples. *Energy Fuels* **2008**, *22*, 3265–3274.

(63) Putman, J. C.; Moulian, R.; Barrère-Mangote, C.; Rodgers, R. P.; Bouyssiere, B.; Giusti, P.; Marshall, A. G. Probing Aggregation Tendencies in Asphaltenes by Gel Permeation Chromatography. Part 1: Online Inductively Coupled Plasma Mass Spectrometry and Offline Fourier Transform Ion Cyclotron Resonance Mass Spectrometry. *Energy Fuels* **2020**, *34*, 8308–8315.

(64) Carbognani, L.; Rogel, E. Solvent Swelling of Petroleum Asphaltenes. *Energy Fuels* **2002**, *16*, 1348–1358.

(65) Carbognani, L.; Rogel, E. Solid Petroleum Asphaltenes Seem Surrounded by Alkyl Layers. *Pet. Sci. Technol.* **2003**, *21*, 537–556.

(66) Stachowiak, C.; Vigié, J.-R.; Grolier, J.-P. E.; Rogalski, M. Effect of N-Alkanes on Asphaltene Structuring in Petroleum Oils. *Langmuir* **2005**, *21*, 4824–4829.

(67) Alawani, N. A.; Panda, S. K.; Lajami, A. R.; Al-Qunaysi, T. A.; Muller, H. Characterization of Crude Oils through Alkyl Chain-Based Separation by Gel Permeation Chromatography and Mass Spectrometry. *Energy Fuels* **2020**, *34*, 5414–5425.

(68) Panda, S. K.; Alawani, N. A.; Lajami, A. R.; Al-Qunaysi, T. A.; Muller, T. Characterization of Aromatic Hydrocarbons and Sulfur Heterocycles in Saudi Arabian Heavy Crude Oil by Gel Permeation Chromatography and Ultrahigh Resolution Mass Spectrometry. *Fuel* **2019**, *235*, 1420.

(69) Putman, J. C.; Moulian, R.; Smith, D. F.; Weisbrod, C. R.; Chacón-Patiño, M. L.; Corilo, Y. E.; Blakney, G. T.; Rumancik, L. E.; Rodgers, C. P.; Giusti, P.; et al. Probing Aggregation Tendencies in Asphaltenes by Gel Permeation Chromatography. Part 2: Online Inductively Coupled Plasma Mass Spectrometry and Offline Fourier Transform Ion Cyclotron Resonance Mass Spectrometry. *Energy Fuels* **2020**, *34*, 10915.

(70) Molnárné Guricza, L.; Schrader, W. Optimized Asphaltene Separation by Online Coupling of Size Exclusion Chromatography and Ultrahigh Resolution Mass Spectrometry. *Fuel* **2018**, *215*, 631–637.

(71) Smith, D. F.; Podgorski, D. C.; Rowland, S. M.; Hendrickson, C. L. 21 Tesla FT-ICR Mass Spectrometer for Complex Mixture Analysis. *Proceedings of the ASMS Asilomar Conference 2016 Pacific Grove, CA, USA, October 14–18, 2016*.

(72) Chacón-Patiño, M. L.; Vesga-Martínez, S. J.; Blanco-Tirado, C.; Orrego-Ruiz, J. A.; Gómez-Escudero, A.; Combariza, M. Y. Exploring Occluded Compounds and Their Interactions with Asphaltene Networks Using High-Resolution Mass Spectrometry. *Energy Fuels* **2016**, *30*, 4550–4561.

(73) Giraldo-Dávila, D.; Chacón-Patiño, M. L.; McKenna, A. M.; Blanco-Tirado, C.; Combariza, M. Y. Correlations between Molecular Composition and Adsorption, Aggregation, and Emulsifying Behaviors of PetroPhase 2017 Asphaltenes and Their Thin-Layer Chromatography Fractions. *Energy Fuels* **2018**, *32*, 2769.

(74) Chacón-Patiño, M. L.; Smith, D. F.; Hendrickson, C. L.; Marshall, A. G.; Rodgers, R. P. Advances in Asphaltene Petroleomics. Part 4. Compositional Trends of Solubility Subfractions Reveal That

Polyfunctional Oxygen-Containing Compounds Drive Asphaltene Chemistry. *Energy Fuels* **2020**, *34*, 3013–3030.

(75) Gascon, G.; Vargas, V.; Feo, L.; Castellano, O.; Castillo, J.; Giusti, P.; Acavedo, S.; Lienemann, C.-P.; Bouyssiere, B. Size Distributions of Sulfur, Vanadium, and Nickel Compounds in Crude Oils, Residues, and Their Saturate, Aromatic, Resin, and Asphaltene Fractions Determined by Gel Permeation Chromatography Inductively Coupled Plasma High-Resolution Mass Spectrometry. *Energy Fuels* **2017**, *31*, 7783–7788.

(76) Kaiser, N. K.; Savory, J. J.; Hendrickson, C. L. Controlled Ion Ejection from an External Trap for Extended m/z Range in FT-ICR Mass Spectrometry. *J. Am. Soc. Mass Spectrom.* **2014**, *25*, 943–949.

(77) Blakney, G. T.; Hendrickson, C. L.; Marshall, A. G. Predator Data Station: A Fast Data Acquisition System for Advanced FT-ICR MS Experiments. *Int. J. Mass Spectrom.* **2011**, *306*, 246–252.

(78) Corilo, Y. E. *PetroOrg Software*; Florida State University; all rights reserved, 2013. <http://www.petroorg.com>.

(79) Putman, J. C.; Moulian, R.; Smith, D. F.; Weisbrod, C. R.; Chacón-Patiño, M. L.; Corilo, Y. E.; Blakney, G. T.; Rumancik, L. E.; Barrère-Mangote, C.; Rodgers, R. P.; et al. Probing Aggregation Tendencies in Asphaltenes by Gel Permeation Chromatography. Part 2: Online Detection by Fourier Transform Ion Cyclotron Resonance Mass Spectrometry and Inductively Coupled Plasma Mass Spectrometry. *Energy Fuels* **2020**, *34*, 10915–10925.

(80) Acevedo, N.; Moulian, R.; Chacon-Patino, M. L.; Mejia, A.; Radji, S.; Daridon, J.-L.; Mangote, C.; Giusti, P.; Rodgers, R. P.; Piscitelli, V.; et al. Understanding Asphaltene Fraction Behavior through Combined Quartz Crystal Resonator Sensor, FT-ICR MS, GPC ICP HR-MS and AFM Characterization. Part I: Extrography Fractionations. *Energy Fuels* **2020**, *34*, 13903.

(81) Kalli, A.; Smith, G. T.; Sweredoski, M. J.; Hess, S. Evaluation and Optimization of Mass Spectrometric Settings during Data-Dependent Acquisition Mode: Focus on LTQ-Orbitrap Mass Analyzers. *J. Proteome Res.* **2013**, *12*, 3071–3086.

(82) Zhao, X.; Shi, Q.; Gray, M. R.; Xu, C. New Vanadium Compounds in Venezuela Heavy Crude Oil Detected by Positive-Ion Electrospray Ionization Fourier Transform Ion Cyclotron Resonance Mass Spectrometry. *Nature* **2014**, *4*, 5373.

(83) Qian, K.; Fredriksen, T. R.; Mennito, A. S.; Zhang, Y.; Harper, M. R.; Merchant, S.; Kushnerick, J. D.; Rytting, B. M.; Kilpatrick, P. K. Evidence of Naturally-Occurring Vanadyl Porphyrins Containing Multiple S and O Atoms. *Fuel* **2019**, *239*, 1258–1264.

(84) Putman, J. C.; Rowland, S. M.; Corilo, Y. E.; McKenna, A. M. Chromatographic Enrichment and Subsequent Separation of Nickel and Vanadyl Porphyrins from Natural Seeps and Molecular Characterization by Positive Electrospray Ionization FT-ICR Mass Spectrometry. *Anal. Chem.* **2014**, *86*, 10708–10715.

(85) Lin, Y.-J.; Cao, T.; Chacón-Patiño, M. L.; Rowland, S. M.; Rodgers, R. P.; Yen, A.; Biswal, S. L. Microfluidic Study of the Deposition Dynamics of Asphaltene Subfractions Enriched with Island and Archipelago Motifs. *Energy Fuels* **2019**, *33*, 1882–1891.

(86) Evdokimov, I. N.; Fesan, A. A.; Losev, A. P. Occlusion of Foreign Molecules in Primary Asphaltene Aggregates from Near-UV-Visible Absorption Studies. *Energy Fuels* **2017**, *31*, 1370–1375.

(87) Milordov, D. V.; Usmanova, G. S.; Yakubov, M. R.; Yakubova, S. G.; Romanov, G. V. Comparative Analysis of Extractive Methods of Porphyrin Separation from Heavy Oil Asphaltenes. *Chem. Technol. Fuels Oils* **2013**, *49*, 232–238.

(88) Dechaine, G. P.; Gray, M. R. Chemistry and Association of Vanadium Compounds in Heavy Oil and Bitumen, and Implications for Their Selective Removal. *Energy Fuels* **2010**, *24*, 2795–2808.

(89) Novelli, J. M.; Medina, J. C.; Lena, L.; Ruiz, J. M.; Vincent, E. J. Vanadium in Heavy Petroleum Crudes. *Collect. Colloq. Semin. (Inst. Fr. Pet.)* **1984**, *40*, 169–172.

(90) McKenna, A. M.; Purcell, J. M.; Rodgers, R. P.; Marshall, A. G. Identification of Vanadyl Porphyrins in a Heavy Crude Oil and Raw Asphaltene by Atmospheric Pressure Photoionization Fourier Transform Ion Cyclotron Resonance (FT-ICR) Mass Spectrometry. *Energy Fuels* **2009**, *23*, 2122–2128.

(91) Ali, M. F.; Perzanowski, H.; Bukhari, A.; Al-haji, A. A. Nickel and Vanadyl Porphyrins in Saudi Arabian Crude Oils. *Energy Fuels* **1993**, *7*, 179–184.

(92) Qian, K.; Edwards, K. E.; Mennito, A. S.; Walters, C. C.; Kushnerick, J. D. Enrichment, Resolution, and Identification of Nickel Porphyrins in Petroleum Asphaltene by Cyclograph Separation and Atmospheric Pressure Photoionization Fourier Transform Ion Cyclotron Resonance Mass Spectrometry. *Anal. Chem.* **2010**, *82*, 413–419.

(93) Rosell-Melé, A.; Maxwell, J. R. Rapid Characterization of Metallo Porphyrin Classes in Natural Extracts by Gel Permeation Chromatography/Atmospheric Pressure Chemical Ionization/Mass Spectrometry. *Rapid Commun. Mass Spectrom.* **1996**, *10*, 209–213.

(94) Biggs, W. R.; Fetzer, J. C.; Brown, R. J.; Reynolds, J. G. Characterization of Vanadium Compounds in Selected Crudes I. Porphyrin and Non-Porphyrin Separation. *Liq. Fuels Technol.* **1985**, *3*, 397–421.

(95) Zhao, X.; Shi, Q.; Gray, M. R.; Xu, C. New Vanadium Compounds in Venezuela Heavy Crude Oil Detected by Positive-Ion Electrospray Ionization Fourier Transform Ion Cyclotron Resonance Mass Spectrometry. *Nature* **2014**, *4*, 5373.

(96) Caumette, G.; Lienemann, C.-P.; Merdrignac, I.; Bouyssiere, B.; Lobinski, R. Element Speciation Analysis of Petroleum and Related Materials. *J. Anal. At. Spectrom.* **2009**, *24*, 263–276.

(97) Reynolds, J. G.; Biggs, W. R. Effects of Asphaltene Precipitation and a Modified D 2007 Separation on the Molecular Size of Vanadium-and Nickel-Containing Compounds in Heavy Residua. *Fuel Sci. Technol. Int.* **1986**, *4*, 749–777.

(98) Mironov, N. A.; Milordov, D. V.; Abilova, G. R.; Yakubova, S. G.; Yakubov, M. R. Methods for Studying Petroleum Porphyrins (Review). *Pet. Chem.* **2019**, *59*, 1077–1091.

(99) Ancheyta, J.; Trejo, F.; Rana, M. S. Definition and Structure of Asphaltenes. *Asphaltene Chemical Transformation during Hydroprocessing of Heavy Oils*; CRC Press, Taylor & Francis Group: Boca Raton, FL, USA, 2010; pp 1–86.

(100) McKenna, A. M.; Marshall, A. G.; Rodgers, R. P. Heavy Petroleum Composition. 4. Asphaltene Compositional Space. *Energy Fuels* **2013**, *27*, 1257–1267.

(101) Ruiz-Morales, Y. HOMO-LUMO Gap as an Index of Molecular Size and Structure for Polycyclic Aromatic Hydrocarbons (PAHs) and Asphaltenes: A Theoretical Study. I. *J. Phys. Chem. A* **2002**, *106*, 11283–11308.

(102) McKenna, A. M.; Chacón-Patiño, M. L.; Weisbrod, C. R.; Blakney, G. T.; Rodgers, R. P. Molecular-Level Characterization of Asphaltenes Isolated from Distillation Cuts. *Energy Fuels* **2019**, *33*, 2018–2029.

(103) Santos Silva, H.; Alfarra, A.; Vallverdu, G.; Bégué, D.; Bouyssiere, B.; Baraille, I. Asphaltene Aggregation Studied by Molecular Dynamics Simulations: Role of the Molecular Architecture and Solvents on the Supramolecular or Colloidal Behavior. *Pet. Sci.* **2019**, *16*, 669–684.

(104) Takanohashi, T.; Sato, S.; Saito, I.; Tanaka, R. Molecular Dynamics Simulation of the Heat-Induced Relaxation of Asphaltene Aggregates. *Energy Fuels* **2003**, *17*, 135–139.

(105) Lobodin, V. V.; Marshall, A. G.; Hsu, C. S. Compositional Space Boundaries for Organic Compounds. *Anal. Chem.* **2012**, *84*, 3410–3416.

(106) Cho, Y.; Kim, Y. H.; Kim, S. Planar Limit-Assisted Structural Interpretation of Saturates/Aromatics/Resins/Asphaltenes Fractionated Crude Oil Compounds Observed by Fourier Transform Ion Cyclotron Resonance Mass Spectrometry. *Anal. Chem.* **2011**, *83*, 6068–6073.

(107) Hsu, C. S.; Lobodin, V. V.; Rodgers, R. P.; McKenna, A. M.; Marshall, A. G. Compositional Boundaries for Fossil Hydrocarbons. *Energy Fuels* **2011**, *25*, 2174–2178.

(108) McKenna, A. M.; Donald, L. J.; Fitzsimmons, J. E.; Juyal, P.; Spicer, V.; Standing, K. G.; Marshall, A. G.; Rodgers, R. P. Heavy Petroleum Composition. 3. Asphaltene Aggregation. *Energy Fuels* **2013**, *27*, 1246–1256.